A REVIEW OF VARIABLES IMPACTING THE INDOOR INHALATION RADON EQUILIBRIUM FACTOR (FEQ)



Kate A. Rodelli Christian M. Salvador Caitlin J. Shanahan Fredrick G. Dolislager APPROVED FOR PUBLIC RELEASE.
DISTRIBUTION IS UNLIMITED.

February 2025



DOCUMENT AVAILABILITY

Reports produced after January 1, 1996, are generally available free via OSTI.GOV.

Website www.osti.gov

Reports produced before January 1, 1996, may be purchased by members of the public from the following source:

National Technical Information Service 5285 Port Royal Road Springfield, VA 22161 *Telephone* 703-605-6000 (1-800-553-6847) *TDD* 703-487-4639 *Fax* 703-605-6900 *E-mail* info@ntis.gov

Website http://classic.ntis.gov/

Reports are available to US Department of Energy (DOE) employees, DOE contractors, Energy Technology Data Exchange representatives, and International Nuclear Information System representatives from the following source:

Office of Scientific and Technical Information PO Box 62
Oak Ridge, TN 37831
Telephone 865-576-8401
Fax 865-576-5728
E-mail reports@osti.gov
Website https://www.osti.gov/

This report was prepared as an account of work sponsored by an agency of the United States Government. Neither the United States Government nor any agency thereof, nor any of their employees, makes any warranty, express or implied, or assumes any legal liability or responsibility for the accuracy, completeness, or usefulness of any information, apparatus, product, or process disclosed, or represents that its use would not infringe privately owned rights. Reference herein to any specific commercial product, process, or service by trade name, trademark, manufacturer, or otherwise, does not necessarily constitute or imply its endorsement, recommendation, or favoring by the United States Government or any agency thereof. The views and opinions of authors expressed herein do not necessarily state or reflect those of the United States Government or any agency thereof.

Environmental Sciences Division

A REVIEW OF VARIABLES IMPACTING THE INDOOR INHALATION RADON EQUILIBRIUM FACTOR (FEQ)

Kate A. Rodelli Christian M. Salvador Caitlin J. Shanahan Fredrick G. Dolislager

February 2025

Prepared by
OAK RIDGE NATIONAL LABORATORY
Oak Ridge, TN 37831
managed by
UT-BATTELLE LLC
for the
US DEPARTMENT OF ENERGY
under contract DE-AC05-00OR22725

CONTENTS

LIS	T OF	FIGURI	ES	IV
LIS	T OF	TABLE	S	V
AC	KNOV	VLEDG	EMENTS	VI
1.	INTI	RODUC	TION	1
2.	IND	OOR IN	HALATION FRACTIONAL EQUILIBRIUM FACTOR (FEQ)	2
3.			URPOSE	
4.			ND ACTINON	
5.				
			GROUND	
	_	5.1.1	UNATTACHED AND ATTACHED RADON PROGENY	
		5.1.2	ATTACHMENT RATE	
		5.1.3	SIZE DISTRIBUTION	
		5.1.4	DEPOSITION RATE	
	5.2		TIONSHIPS WITH FEQ	
	5.3		FIC AEROSOL SOURCES	
	0.0	5.3.1	INDOOR-OUTDOOR EXCHANGE OF AIR POLLUTION	
		5.3.2	CIGARETTE SMOKING	
		5.3.3	ELECTRONIC CIGARETTES	
		5.3.4	CANDLES	
		5.3.5	COOKING	
6.	RHI		SPECIFIC CHARACTERISTICS	
0.	6.1		LEANING METHODS	
	0.1	6.1.1	COMPARISONS OF CLEANING METHODS	
		6.1.2	PUREFLOW AIR TREATMENT SYSTEM	
	6.2		TLATION SYSTEMS	
	6.3		VE AND INACTIVE HOURS	
	6.4		CTURAL FEATURES	
	0.4	6.4.1		
		6.4.2	BUILDING MATERIALS	
		6.4.3	WALL COVERINGS	
		6.4.4	FLOOR LEVEL	
7.	ENIX	O	MENTAL AND METEOROLOGICAL CONDITIONS	
/.	7.1		TIVE HUMIDITY	_
	7.1		PERATURE AND SEASONAL VARIATION	
	7.2		IPITATION AND BAROMETRIC PRESSURE	
			OGICAL AND TOPOGRAPHIC FACTORS	
8.	7.4		N	
٥.				30
	8.1	SOM	MARY OF THE IMPACT OF AEROSOLS, AIR CLEANING, AND RONMENTAL CONDITIONS	20
	0.2	EINVII	RE APPLICATIONS TO RVISL CALCULATOR	21
	8.2			
	8.3		RE RESEARCH	
		8.3.1	AEROSOLS	
		8.3.2	AIR CLEANING SYSTEMS	
0	DEE	8.3.3	ENVIRONMENTAL AND BUILDING-SPECIFIC CHARACTERISTICS	
9.			ES	
			UTDOOR F _{EQ} XHALATION AND EMANATION	
API	~HIVII)	IX R F	XHALATION AND EMANATION	H-I

LIST OF FIGURES

Figure 1. Simplified overview of the formation of clusters and attachment of progeny to an	
aerosol particle	9
Figure 2 The variation of F _{eq} based on varying mass loading of indoor air aerosols produced (e.g.	
cooking, candle lighting, and smoking) and removed (e.g., air purifier) by different	
indoor events.	31
Figure 3. Percentage increase in the Rn-222 F _{eq} due to elevated indoor aerosol concentrations	
from smoking	32
Figure 4. Percentage decrease in the Rn-222 F _{eq} due to the presence of air-cleaning systems	33

LIST OF TABLES

Table 1. Summary of current suggested radon levels in dwellings and corresponding equilibrium	
factors (F _{eq}) of Rn-222, Rn-220, and Rn-219	5
Table 2. Summary of current suggested radon levels in commercial/occupational settings and	
corresponding equilibrium factors (F _{eq}) of Rn-222 and Rn-220	6
Table 3. Diameter ranges for unattached and attached progeny (nm)	10
Table 4. Diameter ranges for modes (nm)	12
Table 5. Aerosol sources and resulting F _{eq} values	16
Table 6. Building-specific characteristics and associated F _{eq} values	23
Table 7. Environmental conditions and resulting F _{eq} values	28
Table 8. Outdoor Rn-220 and Rn-222 F _{eq} values	A-3
Table 9. Exhalation rates of Rn-222 and Rn-220 from various mediums (mBq m ⁻² s ⁻¹)	B-4
Table 10. Emanation power of Rn-222 and Rn-220 from various mediums (ε)	
Table 11. Ra-226 concentration in various mediums (Bq kg ⁻¹)	

ACKNOWLEDGEMENTS

The authors extend their gratitude to Dellaney Bellis for her artistic contributions and to Debra Stewart for her expertise in technical editing. Their invaluable contributions greatly enhanced the communication of our findings.

ABSTRACT

With radon and its daughter products estimated as the second leading cause of lung cancer in the United States, it is imperative to understand their relative equilibrium inside commercial, community, and residential dwellings. The radon indoor inhalation fractional equilibrium factor (F_{eq}) quantifies the disequilibrium between radon and its progeny in indoor air, and recent advances have shown how air exchange rates (ACH) influence F_{eq} . These numerically derived ACH-dependent F_{eq} values are incorporated into the U.S. EPA's Radon Vapor Intrusion Screening Level (RVISL) calculator, which assists risk assessors in evaluating radon exposure. To advance the risk assessment science of actinon (Rn-219), thoron (Rn-220), and radon (Rn-222), the impact of variables such as indoor aerosol concentration and composition, outdoor air quality, household-specific characteristics, and environmental/meteorological conditions on the F_{eq} must be examined. The primary objective of this research is to analyze these additional variables to determine the usefulness of incorporating such adjustment factors into the RVISL calculator and to identify areas of future research.

Studies regarding the influence of these parameters are presented along with recommendations regarding the adjustment of the numerically derived F_{eq} value. For example, elevated indoor aerosol concentrations, such as those originating from outdoor $PM_{2.5}$ or cigarette smoke, increase the abundance of accumulation-mode particles indoors, which in turn raises F_{eq} values by facilitating the attachment of radon progeny to these aerosols. Smoking increases both the bronchial dose and F_{eq} , while regions with high smog levels demonstrate the impact of regional air quality on F_{eq} . In contrast, air cleaning systems and purifiers have been shown to reduce the F_{eq} , suggesting that these systems could help mitigate radon exposure. Additionally, higher F_{eq} values are typically observed during winter when ventilation rates are lower. This paper presents adjustment factors that may be applied to the RVISL F_{eq} , emphasizing the need for further research to refine these variables and ensure accurate risk assessments in diverse environments. Applying these adjustment factors will minimize calculator over- and underestimations, providing a more accurate representation of the real-world risk associated with radon.

1. INTRODUCTION

Radon (Rn-222), the most frequently studied radioactive gas, is a naturally occurring inert gas primarily produced as part of the decay chain of the uranium-238 (U-238) isotope (Nero et al., 1990). Radon is commonly found in radioactive ore located in bedrock, soil, and groundwater aquifers with trace concentrations of U-238 (Nero et al., 1990). Through the natural processes of emanation and exhalation, radon vapors are released from solid mineral grains into air-filled pores in soil, rock, and building materials, subsequently entering indoor or outdoor air (See Appendices A&B) (Collé et al., 1981). Thoron (Rn-220) is a product of the decay chain of the thorium-232 (Th-232) isotope, and Actinon (Rn-219) is a product of the decay chain of the actinium-227 (Ac-277) isotope. Radium-226 (Ra-226), radium-224 (Ra-224), and radium-223 (Ra-223) undergo alpha decay to form Rn-222, Rn-220, and Rn-219, with alpha-decay energies of 4.87 MeV, 5.79 MeV, and 5.98 MeV, respectively (Vaupotič, 2024; National Nuclear Data Center (NNDC), 2020).

Understanding these radioactive decay chains is crucial to assess the health risks of short-lived radon progeny, which are responsible for radon being the second leading cause of lung cancer in the United States (Carmona, 2005; Chu & Liu, 1996). The toxicity and dosimetry of radon gas are lower than those of its short-lived decay products, primarily due to the shorter residence time of noble gases in lung tissue compared to their progeny. The cancer risk and bronchial dose can be attributed to progeny from the radon decay chain depositing onto lung tissue and emitting a harmful dose of radioactive alpha particles (Jasaitis & Girgždys, 2013). The exposure to the progeny in air is often measured in working levels (WL), defined as the combination of short-lived radon decay products per liter of air that results in a total alpha particle emission with energy equaling that of 130 billion electron volts (US CFR, 2021). Thoron and radon WL standards for the Uranium Mill Tailings Radiation Control Act of 1978 are set at 0.02, and there is no WL standard for Rn-219. In the case of Rn-222, only progeny before Pb-210 are included; Pb-210 has a 22.2year half-life and will not be airborne to continue generating progeny available for inhalation. For Rn-220 and Rn-219, all progeny are included. Contributing to these WL calculations is the time in which decay occurs. Actinon, thoron, and radon have half-lives of 3.96 seconds, 55.6 seconds, and 3.82 days, respectively (United States Environmental Protection Agency (US EPA), 2023a). Lead-212 (Pb-212) is a decay product of thoron with a notably longer half-life of 10.6 hours; however, all the Rn-220 progeny are included in radon indoor inhalation fractional equilibrium factor (F_{eq}) and WL calculations (US EPA, 2023a).

The radon indoor inhalation fractional equilibrium factor (F_{eq}) is used to convert from concentration (pCi) to WL and vice versa, enabling comparisons to State and Federal standards. The F_{eq} is a unitless measurement of the disequilibrium associated with the decay of the parent and its subsequent progeny in a specified volume. Recent advances in understanding how air exchange (ACH) rates impact F_{eq} have led to the implementation of numerically derived, ACH-dependent F_{eq} values used in the United States Environmental Protection Agency's radon vapor intrusion screening level (RVISL) calculator (US EPA, 2023b; ORNL, 2022). The goal of the RVISL calculator is "to assist risk assessors, remedial project managers, on-scene coordinators, and others involved with risk assessment and decision-making at Comprehensive Environmental Response, Compensation, and Liability Act (CERCLA) sites in developing RVISLs" or preliminary remediation goals (PRGs) for indoor Rn-222, Rn-220, and Rn-219 that are working level, risk, or dose based (US EPA, 2023a, pp. 1-2). The numerically derived F_{eq} values do not consider many site-specific factors that can modify the F_{eq} . Therefore, it is crucial to investigate how indoor aerosol concentration and composition, outdoor air quality, household characteristics, and environmental/meteorological factors influence the F_{eq} to enable more accurate RVISL outputs.

2. INDOOR INHALATION FRACTIONAL EQUILIBRIUM FACTOR (FEQ)

 F_{eq} is a unitless measurement of the disequilibrium associated with the decay of the parent and its subsequent progeny. It is useful in calculating the detriment from inhalation of radon progeny, as most of the dose received is from the progeny rather than the parent. Therefore, the dose per unit radon gas activity is greatly dependent on the state of equilibrium of the decay products with their parent (Centers for Disease Control and Prevention (CDC), 2018). The equation for F_{eq} is:

$$(F_{eq})_i = \frac{Progeny\ PAEC}{Progeny\ PAEC\ at\ Equilibrium}$$
 [1]

where i represents an arbitrary air exchange rate. The progeny potential alpha energy concentration (PAEC) in the numerator of equation [1] may be calculated at any air exchange rate. The progeny PAEC in the denominator of equation [1] is at a state of equilibrium, where no air exchanges are taking place. When there is no air exchange, the numerator and denominator of equation [1] are equal, and F_{eq} has a value of one. As the air exchange rate in a specified volume increases, F_{eq} decreases and vice-versa. F_{eq} is only defined for decay chains that contain alpha-emitting progeny.

The potential alpha energy (PAE) of a nuclide is defined as the total amount of energy emitted through alpha particles as the nuclide decays to a stable isotope (or, for this paper, a sufficiently long-lived isotope). If a decay chain has multiple possible paths, the PAE is an average of the energy released by those paths, weighted by the probability of each path. When radioactive particles deposit inside the respiratory system, they will proceed to decay through their full chain; thus, the PAE of a particle represents how much damage it will cause when inhaled. It is also helpful to talk about PAEC, the concentration of PAE in a volume. The DOE Standard only defines PAEC and gives the weighting coefficients for the thoron and radon decay chains. For a mixture of isotopes (as in the case of a suspended decay chain), the PAEC is simply a sum of the PAECs for each individual isotope. The PAEC for some isotope, k, is given in equation [2] below, where C_k is the activity concentration and t_{-k} is the half-life.

$$PAEC_k = \frac{t_{\frac{1}{2}k}PAE_k}{\ln{(2)}}C_k \qquad [2]$$

Determining the PAE for each isotope was done as follows. For a nuclide A, which decays into nuclides B (b decay probability, decay alpha energy = 0) and C (c decay probability, decay alpha energy = α), the PAE is given by:

$$PAE_A = b(PAE_B + 0) + c(PAE_C + \alpha)$$
 [3]

Equation [3] was applied recursively, starting at the bottom of the decay chain (stable and long-lived isotopes) with PAE = 0 and then working upwards.

 F_{eq} is only used in the conversions of working levels to concentration and is presented in the calculator output (EPA, 2023b). The conversion equation is:

$$C_{res-ia-inh}\left(\frac{pCi}{L}\right) = \left(\frac{TWL}{\left(F_{eq} \times \frac{1WL}{Ceq}\right)}\right)$$
 [4]

Here, TWL is the target working level and C_{eq} is a constant representing what concentration of the parent gas equates to 1 WL at equilibrium, in units of picocuries per liter, per working level. C_{eq} equals 162 pCi/L for actinon, 7.5 pCi/L for thoron, and 100 pCi/L for radon.

Historically, F_{eq} was used to describe the disequilibrium of the progeny in air and was significant in evaluating the risk and dose. F_{eq} has been researched for thoron and radon in various dwellings for many years (Chen & Harley, 2018).

3. PROJECT PURPOSE

The purpose of this project is to identify future research needs that would help define additional factors, other than ACH, that can be applied to the F_{eq} to reduce uncertainty and estimation by the RVISL calculator. According to the US EPA's RVISL user guide, the F_{eq} acts as a conversion factor to determine local, state, federal, and international compliance with WL-based applicable or relevant and appropriate requirements (ARARs) issued under the Uranium Mill Tailings Radiation Control Act (UMTRCA) in addition to risk-based limits and dose-based limits that are ARARs (US EPA, 2023a). It is well understood that the F_{eq} is largely influenced by ventilation, as air exchanges result in a complete renewal of indoor air. Lesser studied factors include air quality, particulate matter concentration and composition, seasonal variation, and other building-specific and environmental conditions. These factors will be discussed in this paper.

Tables 1 and 2 present current regulatory and recommended indoor radon concentrations from several regulatory agencies and the reported F_{eq} values. There is no current UMTRCA standard for Rn-219. For Rn-222 and Rn-220, the standard of 0.02 WL is used as an ARAR. Previously, an assumed F_{eq} of 0.4 (40%) for Rn-222 and 0.02 (2%) for Rn-220 was used. When applying these standards to equation [4], the ARAR compliance level was 5 pCi L⁻¹ or 187 Bq m⁻³ for Rn-222 and 7.5 pCi L⁻¹ or 277.5 Bq m⁻³ for Rn-220 (US EPA, 2023a), although that has been superseded with the issuance of the RVISL and its new F_{eq} values

Table 1. Summary of current regulatory and recommended radon levels in dwellings and corresponding equilibrium factors (Feq) of Rn-222, Rn-220, and Rn-219

	RADON (RN-222)			THORON (RN-220)			ACTINON (RN-219)			
Source	Concentration (pCi L ⁻¹)	Concentration (Bq m ⁻³)	F_{eq}	Concentration (pCi L ⁻¹)	Concentration (Bq m ⁻³)	F_{eq}	Concentration (pCi L ⁻¹)	Concentration (Bq m ⁻³)	F_{eq}	
US Environmental Protection Agency (US EPA) ^a	4	148	-	-	-	-	-	-	-	
Uranium Mill Tailings Radiation Control Act (UMTRCA) ^b	5	185	0.4	7.5	277.5	0.02	-	-	-	
International Commission on Radiological Protection (ICRP) Indoor Standard ^c	2.7 - 8.1	100 - 300	0.4	-	-	-	-	-	-	
National Council on Radiation Protection and Measurements (NCRP) ^d	8-10	296 - 370	0.4-0.5	-	-	-	-	-	-	
Oak Ridge National Laboratory (ORNL) Resident ^c	-	-	0.8683	-	-	0.2609	-	-	0.8645	
Oak Ridge National Laboratory (ORNL) Commercial ^e	-	-	0.6599	-	-	0.09396	-	-	0.6564	
United Nations Scientific Committee on The Effects of Atomic Radiation (UNSCEAR) ^f	-	-	0.4	-	-	-	-	-	-	
World Health Organization (WHO)g	2.7	100	1	-	-	-	-	-	-	
European Environment & Health Information System (ENHIS) ^h	5.4 – 10.8	200 - 400	-	-	-	-	-	-	-	
Commission of the European Communities (CEC) ^d	10.8	400	-	-	-	-	-	-	-	
Nordic Radiation Protection Institutes (NRPI) ^d	10.8	400	-	-	-	-	-	-	-	
Health Canada ⁱ	5.4	200	1	-	-	1	-	-	-	

Concentrations in italics were converted using 1 pCi = 0.037 Bq. Values come from: aUS EPA, 2016; bUS EPA, 2014; cICRP, 2010; dNational Research Council (US), 1999; cORNL, 2022; fUNSCEAR, 2000; gWHO, 2010; bENHIS & WHO, 2005; Health Canada, 2017.

Table 2. Summary of current regulatory and recommended radon levels in commercial/occupational settings and corresponding equilibrium factors (F_{eq}) of Rn-222 and Rn-220

Source		RADON (RN-222)	THORON (RN-220)						
Source	Focus	Value	Feq	Comment	Focus	Value	Feq	Comment	
US Environmental Protection Agency ^a	Indoor air (schools, homes, business)	4 pCi	-	Action Level	-	-	-	-	
The Occupational Safety and Health Administration (OSHA) b	Occupational	4 WLM year ⁻¹	-	Regulation	-	-	-	-	
National Institute for Occupational Safety and Health (NIOSH) ^c	Mining	1 WLM year-1	-	Guidance	-	-	-	-	
Mine Safety and Health Administration d	Mining	4 WLM year ⁻¹ 1 WL in active mines	-	Regulation	-	-	-	-	
United States Nuclear Regulatory	Annual average effluent	10 pCi L ⁻¹ w/o daughters			Annual average effluent	20 pCi L ⁻¹ w/o daughters			
Commission (USNRC) d	air concentration	0.1 pCi L ⁻¹ w/ daughters	-	-	air concentration	0.03 pCi L ⁻¹ w/ daughters	-	-	
Department of Energy (DOE) d	Occupational (DOE)	10 WLM year ⁻¹	-	Regulation	-	-	-	-	
International Atomic Energy Agency (IAEA) ^d	Aboveground Workplace	1,000 Bq m ⁻³	-	Action Level	-	-	-	-	
	Indoor Workplaces	20 mSv WLM ⁻¹	0.4		Indoor Workplaces	5.6 mSv WLM ⁻¹		Effective	
International Commission on Radiological Protection (ICRP) ^e	Mining	12 mSv WLM ⁻¹	0.4	Effective Dose per Exposure	Mining 1/2 mSy W/1		-	- Dose per	
(1010)	Tourist Caves	24 mSv WLM ⁻¹	0.2	F == ===P 000070	-	-		Exposure	

Values come from: a US EPA, 2024d; b OSHA, 2021; Agency for Toxic Substances and Disease Registry (ATSDR), 2010; Daniels & Schubauer-Berigan, 2018; Paquet et al., 2017.

4. THORON AND ACTINON

For the purposes of this project, actinon (Rn-219), thoron (Rn-220), and radon (Rn-222) are all considered. Actinon and thoron are decay products of actinium-227 and thorium-232, respectively. Relevant information on factors influencing the F_{eq} of Rn-219 (actinon) was not found, and data on the Rn-220 F_{eq} was limited compared to Rn-222. This highlights the need for further research in these areas.

Due to the short half-life of thoron (Rn-220) (55.6 seconds), thoron in the soil beneath a building typically does not survive long enough to enter and accumulate indoors (Chen & Harley, 2018). Only exceptionally high levels of Rn-220 in soil or outdoor air result in high concentrations in indoor environments (Vaupotič, 2024). Therefore, prior research predominantly focused on factors influencing Rn-222, as Rn-220 was thought to contribute insignificantly to the health risk. However, recent studies reported higher Rn-220 levels indoors, generally attributed to exhalation from thorium present in building materials (Vaupotič, 2024; Chen & Harley, 2018; Kolarž et al., 2017). Thoron progeny contribution to dose was measured at 7% in Canadian homes (Chen & Marro, 2011) and up to 20% throughout indoor environments in India (Ramachandan & Sathish, 2011).

Because of the differences in half-life between Rn-222 and Rn-220, radon and thoron activity concentrations behave differently indoors. In a closed room, Rn-222 activity concentration is assumed to be distributed uniformly. On the other hand, the activity concentration of Rn-220 decreases exponentially with increasing distance from the exhalation surface (Vaupotič, 2024; Kolarž et al., 2017). For instance, Rn-220 activity decreased rapidly within 10 to 20 cm from its source, reaching a uniform distribution in the typical breathing zone in a study by Chen & Harley (2018). Under steady-state conditions, the thoron activity concentration was calculated to be less than 1% of its value at the wall surface (Chen & Harley 2018). However, recent measurements indicate that circulating air currents in typical indoor environments result in higher thoron activity concentrations at distances further from their sources. Unlike radon activity concentration, which decreases with increasing ventilation rates, higher ventilation rates increase the thoron activity concentration measured in the typical breathing zone, as activity is distributed throughout the indoor environment (Vaupotič, 2024; Ramola et al., 2005). Regardless, measurements of thoron gas and decay products for human exposure assessment should be made in the typical breathing zone (Chen & Harley, 2018).

A thoron study measuring F_{eq} in 113 Canadian homes found a geometric mean of 0.022, consistent with the EPA value of 0.02. Measurements of F_{eq} from 3,869 dwellings, offices, and schools across 13 countries and regions showed variation in the Rn-220 F_{eq} from 0.003 to 0.14, with a mean of 0.042 and a standard deviation of 0.031 (Chen & Harley, 2018). The wide range of measured F_{eq} values suggests that location-specific values measured in the typical breathing zone are more appropriate for calculating lung bronchial dose than a worldwide average value (Chen & Harley, 2018). Another study proposed that thoron dose estimates should be based on direct measurements of thoron progeny concentrations (Prasad et al., 2023). Further research into emanation rates and Rn-220 gas concentrations may prove more valuable for dose calculations than F_{eq} .

5. AEROSOLS

5.1 BACKGROUND

A discussion on the relevant properties of aerosols and fundamentals of radon and thoron decay products will be provided to supply essential background information pertinent to F_{eq} . The addition of aerosol science to the analysis of radon and thoron decay products in indoor environments is relatively new. However, existing literature demonstrates that aerosol concentration and composition significantly influence F_{eq} , highlighting the need for comprehensive investigations into aerosol dynamics to develop precise adjustment factors for tools like the RVISL calculator.

5.1.1 Unattached and Attached Radon Progeny

Po-218, Pb-214, Bi-214, and Po-214 are the short-lived decay products of Rn-222 that have a significant impact on human health, as these non-gaseous progenies represent the largest fraction of natural radiation exposure in humans (Porstendörfer, 1994; Chu & Liu, 1996). After undergoing alpha-decay, 85-90% of the newly formed radionuclides are positive ions (Mostafa et al., 2020) that react with molecules of trace gases and water vapor to neutralize and form small positive or neutral clusters (Chu & Liu, 1996; Hopke, 1996). These newly formed radionuclides and clusters are called unattached progeny, defined by their lack of attachment to aerosol particles and primarily classified by their size (0.5 - 5 nanometers) (Jasaitis & Girgždys, 2013; Porstendörfer, 1994). In addition to cluster formation and neutralization, unattached progeny attach to aerosols present in the ambient air and appear as radioactive aerosols. Aerosols are suspended particles or liquids in gas and can have natural or anthropogenic sources, varying widely in their composition, size, and concentration (Seinfeld and Pandis, 2016). These radioactive aerosols are known as attached progeny, characterized by a larger size distribution (5 -3000 nm) (Jasaitis & Girgždys, 2013; Porstendörfer, 1994). However, existing literature conflicts regarding the exact size ranges of unattached and attached progeny, which can be seen in Figure 1 and Table 3. Generally, the larger, attached fraction and the smaller, unattached fraction explain the bimodal size distribution of radon progeny indoors (Chu & Liu, 1996).

The unattached fraction (f) is a unitless value representing the amount of radon progeny not attached to aerosols (Yu et al., 1996) and is determined by the aerosol-attachment rate and the deposition rate on walls and other surfaces of a room (Reineking & Porstendörfer, 1990). Quantifying unattached and attached radionuclides is important in the development of accurate dosimetry models (Swedjemark & Makitalo, 1990; Mohamed et al., 2008), as the different diffusion rates of these molecules cause activity to settle in distinct regions of the airway and in varying amounts (Mohamad et al., 2008; Jasaitis & Girgždys, 2013). Research illustrates that unattached progeny have a higher bronchial deposition fraction than attached progeny (Mohamed et al., 2014), although this difference does not directly correlate with F_{eq}. The relationship between F_{eq} and (f) requires an exploration of aerosol attachment and deposition and the differences in these processes between unattached and attached progeny.

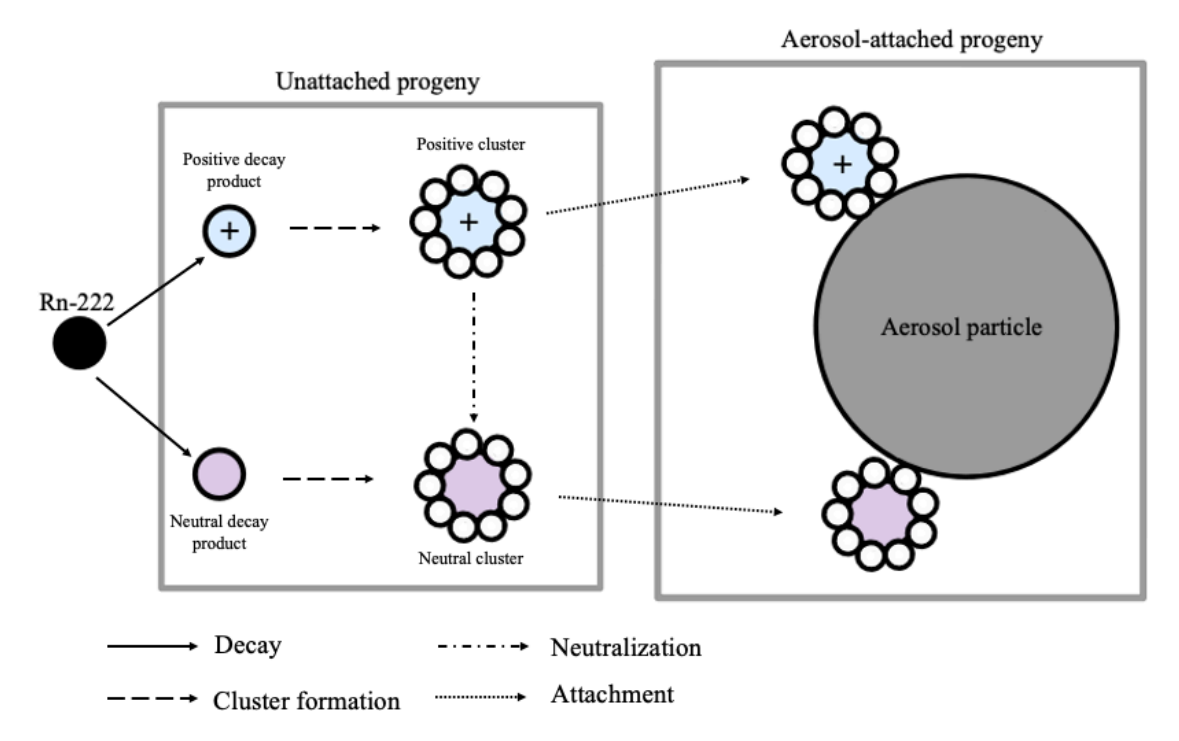


Figure 1. Simplified overview of the formation of clusters and attachment of progeny to an aerosol particle. White circles represent the trace gases and air vapors that partition to the freshly generated radionuclides. Adapted from Fig 3. in Porstendörfer, J. (1994). Properties and behaviour of radon and thoron and their decay products in the air. Journal of Aerosol Science, 25(2), 219-263

5.1.2 Attachment rate

The attachment rate of progeny to aerosols (X, h^{-1}) is proportional to the number concentration of aerosol particles (Z, cm^{-3}) and the size-dependent attachment coefficient $(\beta, cm^3 h^{-1})$ (Porstendörfer, 1994; Vaupotič, 2024). It can be expressed as:

$$X = \beta Z$$
 [5]

Therefore, due to increased aerosol concentration, the attachment rate will be higher in polluted, dusty, or smoky conditions and lower in clean environments (UNSCEAR, 2000). In rooms with ventilation < 0.5 h⁻¹ without any additional aerosol sources, attachment rates were between 20 h⁻¹ and 50 h⁻¹. The addition of aerosol sources increased the attachment rate up to 1000 h⁻¹ (Porstendörfer, 1994; Reineking & Porstendörfer, 1990). Another study discovered that an increase in aerosol particle concentrations up to 260000 # cm⁻³ increased attachment rates up to 3600 h⁻¹ (El-Hussein, 1996).

5.1.3 Size Distribution

Distinctions between number size and activity size distributions are important. Number size distribution (Z(d)) quantifies the number concentration of particles (Z) with regards to diameter (d), without consideration of their radioactive properties. In contrast, the activity size distribution of the decay product p $(C_p(d))$ specifically pertains to decay products and differs from number size distribution because the attachment probability $(\beta(d))$ is a function of particle diameter (Porstendörfer, 1994; Porstendörfer &

Reineking, 2000). The correlation equation between activity and number size distributions can be represented as:

$$\frac{1}{C_p} \frac{\partial C_p(d)}{\partial d} = \frac{\beta(d)}{X} \frac{\partial Z(d)}{\partial d}$$
 [6]

where X is the attachment rate, and C_p is the activity concentration (pCi L⁻¹ or Bq m⁻³) (Porstendörfer & Reineking, 2000). Activity size distribution is modeled with a log-normal size distribution, which is described by the activity median aerodynamic diameter (AMAD) or the activity median diameter (AMD) in nanometers (Porstendörfer, 1994).

5.1.4 Deposition Rate

The deposition rate is the rate at which particles settle out of air and accumulate on surfaces. In general, the deposition rate is dependent on size, with small particles (<10 nm) following Brownian motion, which enhances their deposition rates. The deposition of radon progeny on walls and other surfaces (plate-out) is dependent on deposition velocity. Unattached radon/thoron daughters (0.4 – 0.5 nm) have a deposition velocity about 100 times higher than aerosol-attached progeny (100 – 1000 nm) (Porstendörfer, 1994). Additional research determined that the rate of deposition of the unattached decay product is about 200 times higher than that of aerosol-attached radionuclides (Porstendörfer, 1994). Another study found that the deposition rate was 1 h⁻¹ for ultrafine particles (10 nm diameter) and 0.1 h⁻¹ for particles with a 100 nm diameter (Hussien et al., 2005). Finally, mean deposition rates of unattached and attached progeny were found to be 170 ± 23 h⁻¹ and 0.225 ± 0.092 h⁻¹, respectively (El-Hussein, 1996). Ultimately, evidence consistently shows that unattached progeny deposit onto surfaces at a much higher rate than attached progeny.

Unattached Attached Reference < 4 100 - 400Kranrod et al., 2021 0.5 - 5100 - 1000Porstendörfer, 1994 50 - 500Skubacz & Wołoszczuk, 2019 0.5 - 55 - 3000Jasaitis & Girgždys, 2013 < 10 ~ 100 Hussien et al., 2005 < 5 > 10 Porstendörfer, 2001 0.5 - 1.6Li & Hopke, 1992 0.5 - 1.515 - 500Li & Hopke, 1991 Kranrod et al., 2009 0.5 - 5

Table 3. Diameter ranges for unattached and attached progeny (nm)

5.2 RELATIONSHIPS WITH FEQ

Understanding the unattached fraction (f) and F_{eq} requires knowledge of the relationships between the diameter of the particles, attachment rate, deposition rate, and aerosol concentration. Increased indoor aerosol concentration leads to a higher attachment rate between aerosols and progeny, which subsequently decreases the unattached fraction (Porstendörfer, 1994). As the attachment rate increases, previously unattached progeny bind to aerosols and become attached progeny. Since the deposition rate for unattached progeny is much faster than that of attached progeny, higher attachment rates reduce the overall deposition

rate of progeny onto surfaces. This results in a decrease in the unattached fraction and an increase in F_{eq} (Reineking & Porstendörfer, 1990; Swedjemark, 1983; Porstendörfer, 1994; Jasaitis & Girgždys, 2013), explaining the dependency of the unattached fraction on the attachment rate and the inverse relationship between F_{eq} and (f) (Reineking et al., 1985; Chu & Liu, 1996; El-Hussein, 1996; Jasaitis & Girgždys, 2013). One study determined that the observed decrease in unattached fraction with the addition of aerosol sources was more influenced by attachment rate than aerosol concentration, attributable to variations in the particle size distribution of indoor aerosols from different household sources (Reineking et al., 1985). In contrast, other research established evidence of a direct relationship between (f) and aerosol particle concentration (f = 400/Z) (Vaupotič, 2024).

Further investigations revealed a positively correlating relationship between attachment rate and relative humidity (RH), as aerosol particle size increases with RH, assuming that aerosol components are mostly hydrophilic (Chu & Liu, 1996). Additionally, a study demonstrated the impacts of RH on diffusion coefficients of progeny (Chu & Liu, 1996). Simply put, diffusion coefficients characterize the mobility of progeny in the air (Porstendörfer, 1994). RH impacts the diffusion coefficients of unattached radon daughters in two different ways. First, RH enhances clustering, and the diffusion coefficient decreases as RH increases. Secondly, RH increases the neutralization of Po-218, leading to a higher diffusion coefficient. These effects coexist, but overall, the diffusion coefficient decreases with increasing RH. This leads to a decreased deposition velocity of unattached progeny as RH increases, causing the F_{eq} to increase with increasing RH and demonstrating that the relationship between (f) and F_{eq} is influenced by humidity (Chu & Liu, 1996; El-Hussein, 1996; Porstendörfer, 1994).

Overall, as seen in studies examining houses in real living conditions, theoretical models, and chamber experiments, F_{eq} and (f) are governed by the aerosol conditions of the indoor environment. Increased aerosol concentration increases the attachment rate, which decreases the unattached fraction (El-Hussein, 1996; Reineking & Porstendörfer, 1990). F_{eq} and (f) have an inverse relationship due to the differences in deposition rate between attached and unattached progeny (El-Hussein, 1996; Jasaitis & Girgždys, 2013; Huet et al., 2001). For high attachment rates seen at high aerosol particle concentrations, F_{eq} increased from 0.34 \pm 0.011 to 0.52, and (f) decreased from 0.06 \pm 0.005 to 0.004 (El-Hussein, 1996). However, even at very high aerosol particle concentrations, a F_{eq} of one is not reached because some fraction of progeny is always lost through deposition (Porstendörfer, 1994). Additionally, although enhanced aerosol concentrations increase the attachment rate, the attachment rate is also influenced by particle size, demonstrating the importance of studying the impact that sources and physicochemical properties of aerosols have on F_{eq} (Chu & Liu, 1996; Vaupotič, 2024).

5.3 SPECIFIC AEROSOL SOURCES

Although many studies found a direct correlation between aerosol concentration and F_{eq} (Jasaitis & Girgždys, 2013; Reineking & Porstendörfer, 1990; Porstendörfer, 1994; Wicke, 1981), others suggest that the relationship between aerosol concentration and F_{eq} is only strong when the spread in aerosol particle size distribution is small, as aerosols with different sizes and sources can lead to varying deposition velocities (Chu & Liu, 1996). Although increasing the aerosol concentration generally leads to a lower (f) and higher F_{eq} , the strength of these relationships depends largely on particle size as well as concentration (Huet et al., 2001).

In general, aerosols exhibit a trimodal distribution, characterized by sizes increasing across nucleation mode, accumulation mode, and coarse mode. Aitken mode is sometimes referenced as a size range in between nucleation and accumulation modes, but existing literature conflicts, as illustrated in Table 4. Although the ambient aerosol size in homes is about 100 nm on average, indoor activities and specific aerosol sources modify this average diameter. For example, electric motors, open flames, or electric heaters produce smaller aerosols with diameters around 50 nm, while cigarette smoke produces aerosols about 300

nm in diameter (UNSCEAR, 2000). Importantly, despite variations in the number size distribution of indoor aerosols produced from different sources, the activity size distribution is similar. Activity is primarily attached to particles within the accumulation size range, due to their increased surface area relative to mass (Porstendörfer, 2001; Porstendörfer & Reineking, 2000).

A prior study (Huet et al., 2001) determined that cooking and burning candles resulted in very high aerosol number concentrations (250,000 and 390,000 cm-3, respectively), much higher than those observed from smoking cigarettes. However, the F_{eq} after cooking and burning candles was comparable to the baseline F_{eq} measured when the experiment was run without additional aerosol sources (5000 cm-3). While certain aerosol sources like cooking and candle burning can result in high aerosol number concentrations, the particles produced primarily exist in the nucleation mode, where attachment is lower. Therefore, other indoor activities that produce smaller aerosols (< 50 nm), such as electric motors and heaters (UNSCEAR, 2000), should have less of an impact on F_{eq} . In contrast, the highest F_{eq} values are associated with aerosols in accumulation mode, demonstrating that both aerosol size and concentration impact F_{eq} (Huet et al., 2001). Research investigating the impact of specific aerosol sources is important to increase the accuracy of the F_{eq} . Additional research is needed to examine the size distributions from specific aerosol sources under varying environmental conditions and in the presence of other particle sources. Additionally, the following information pertains specifically to Rn-222, highlighting the necessity for further research on the interactions between aerosol sources and Rn-220 progeny.

Nucleation	Aitken	Accumulation	Coarse	Reference
0.05 - 60	-	60 – 1000	> 1000	Grundel, 2004
3 – 70	-	70 - 2000	2000 – 36000	Kranrod et al., 2021
-	-	100 - 1000	-	Porstendörfer, 2000
-	-	300 - 1000	1000 - 10000	Hussien et al., 2018
10 – 100	-	100 - 1000	-	Mostafa et al., 2011
3 – 20	20 – 100	-	-	Young & Keeler, 2007
< 30	30 – 110	110 - 700	-	Nøjgaard et al., 2012
3 – 12	12 – 60	60 - 1000	> 1000	Williamson et al., 2021

Table 4. Diameter ranges for modes (nm)

5.3.1 Indoor-Outdoor Exchange of Air Pollution

Particulate matter less than 2.5 microns in diameter (PM_{2.5}) can be emitted directly into the air or formed through atmospheric reactions. Major primary sources of PM_{2.5} include emissions from cars, wildfires, woodstoves, cooking, and agricultural operations, while secondary sources include the transformation and oxidation of gas emissions from power plants and industrial processes. PM_{2.5} poses a health risk due to its small size, allowing it to penetrate deep into the lungs and even reach the bloodstream. Additionally, radon daughters can attach to PM_{2.5}, exacerbating the health risk (US EPA, 2024a). While data on the correlation between PM_{2.5} and F_{eq} is limited, existing literature focusing on cities in China and Japan consistently indicates that radon progeny concentrations increase during periods of high PM_{2.5} levels (Hou et al., 2015; Hu et al., 2022; Yu et al., 2023). A broader representation of cities worldwide is crucial for assessing the impacts of PM_{2.5} on F_{eq}. If this research is obtained, the creation of adjustment factors that incorporate air quality index data could refine the RVISL calculator's F_{eq} value.

In China, during the 1980s and 1990s, F_{eq} values ranged between 0.47 and 0.49 (Hou et al., 2015). Since 2013, the number of severely polluted days in China has increased due to frequent haze-fog conditions. A study in Beijing examined F_{eq} values in both urban (Xicheng) and suburban (Changping) areas. They found

that the outdoor concentration of $PM_{2.5}$ significantly impacted indoor $PM_{2.5}$ concentration during haze-fog days. Occupant activity and the opening of windows further increased indoor $PM_{2.5}$ concentrations. During haze-fog days, there was a decrease in the unattached fraction of radon daughters and an increase in aerosol attachment rates. A positive correlation ($R^2 = 0.71$) was observed between indoor F_{eq} values and $PM_{2.5}$ concentration (Hou et al., 2015). Also in Beijing, radon progeny concentrations were positively correlated with increased particulate matter levels from both haze and dust events, with the strongest correlation observed during periods of elevated $PM_{2.5}$ concentrations (Yu et al., 2023). The equilibrium equivalent concentrations of radon (EERC) and thoron (EETC) were measured in three cities in China and Japan to determine their correlation with $PM_{2.5}$ (Hu et al., 2022). EERC and EETC are alternatives to PAEC and are the concentrations of the parent gas "in equilibrium with its progeny that would give the same PAEC as the actual non-equilibrium mixture" (IAEA, n.d.). It was determined that both the EETC and EERC demonstrated a positive correlation with indoor $PM_{2.5}$ concentrations (Hu et al., 2022).

Additionally, research comparing F_{eq} and the unattached fraction in urban and rural Czech dwellings noted a higher F_{eq} in urban settings, as depicted in Table 5. This disparity stems from higher attachment rates in urban dwellings attributed to elevated average aerosol concentrations. The unattached fraction was 0.086 in urban dwellings and 0.107 in rural dwellings, indicating a greater presence of attached progeny in urban air and thereby explaining the observed F_{eq} distinctions (Jílek et al., 2010). Another study compared the F_{eq} for similar dwellings in different locations. The dwellings were categorized based on their proximity to parks/playgrounds, buildings, or roads/work sites. The F_{eq} for dwellings located near playgrounds and parks was significantly lower compared to those near buildings, which in turn was lower than that of dwellings situated near roads and work sites. The lower aerosol concentrations near playgrounds and parks resulted in smaller amounts of attached Rn-222 and Rn-220 progeny, leading to a lower F_{eq} . Conversely, higher aerosol concentrations near roads and work sites resulted in a higher F_{eq} (Yu et al., 1999).

5.3.2 Cigarette Smoking

Research has demonstrated that smoking amplifies the harmful effects of radon. In a setting with the same radon levels, a smoker faces a higher risk of developing cancer from radon exposure compared to a non-smoker. This is because radon progeny settles onto the aerosols emitted from smoking, forming radioactive aerosols that impact the airways (Jasaitis & Girgždys, 2013). The estimated excess lifetime risk of death from radon-induced lung cancer (by age 75) is 0.6×10^{-5} per Bq m-3 for lifelong non-smokers and 15×10^{-5} per Bq m-3 for current smokers (15–24 cigarettes per day). The radon concentrations linked to an excess lifetime cancer risk (ELCR) of 1/100 and 1/1000 are 67 and 6.7 Bq m-3 for current smokers, and 1670 and 167 Bq m-3 for lifelong non-smokers, respectively (WHO, 2010). A study examining 7148 cases of lung cancer and 14208 controls in nine European countries estimated that the relative risk for current smokers was 25.8 times higher than for lifelong non-smokers (Darby et al., 2005).

Cigarettes produce aerosols with size range in the accumulation mode (around 200-300 nm in diameter) (UNSCEAR, 2000; Li & Hopke, 1991). Further research demonstrated that after smoking, the highest contribution to the maximum aerosol concentration came from particles around 100 nm in diameter, followed by those at 70 nm, and then 150 nm (Vaupotič, 2024). A study conducted in Lithuania showed that elevated aerosol particle levels due to smoking led to a heightened attachment rate between unattached radon clusters and aerosol particles, thereby increasing the F_{eq} as depicted in Table 5 (Jasaitis & Girgždys, 2013). The unattached fraction of Po-218 decreased from 0.09 ± 0.02 to 0.03 ± 0.01 in smoke-free and smoke-bearing rooms, respectively. The study identified a positive correlation (r = 0.9) between F_{eq} and aerosol particle concentration along with a negative correlation (r = -0.64) between F_{eq} and the unattached fraction factor (Jasaitis & Girgždys, 2013). Results from another study indicated that aerosol concentrations remained elevated even four hours after smoking, decreasing the unattached fraction from 0.16 to 0.03 and increasing the F_{eq} from 0.36 to 0.60 (Vaupotič, 2024). As a result of the larger particles generated during cigarette smoking, a unimodal activity size distribution between 50 - 500 nm was measured (Li & Hopke,

1991). Because the number size distribution of aerosols generated from cigarettes primarily falls within the accumulation mode, there is a strong relationship between the F_{eq} and smoking, as attachment rates accelerate and surpass the deposition of unattached particles on surfaces (Li & Hopke, 1991). It is important to note that most of these studies were conducted in radon chambers. While chamber studies indicate that aerosols from cigarette smoking increase F_{eq} , these controlled environments do not fully capture the complexities of real-world conditions. There is a critical need for additional field studies to quantify cigarette smoking in terms of cigarettes smoked per day and to understand how these real-world smoking patterns influence F_{eq} . This research is essential for developing adjustment factors for the RVISL calculator that apply to actual smoking scenarios, ensuring the results are relevant and useful for assessing radon exposure in environments where people smoke.

5.3.3 Electronic Cigarettes

Testing conducted in a radon chamber at the Italian National Institute of Ionizing Radiation Metrology examined the interaction between aerosols released from electronic cigarettes and radon progeny, comparing these results with those of traditional cigarettes (Trassierra et al., 2015; Vaupotič, 2024). Like aerosols from traditional cigarettes, electronic cigarette aerosols act as carriers for radon progeny, reducing the deposition of radon daughters and thus increasing the F_{eq}. Despite traditional cigarettes resulting in a higher particle concentration and a slightly lower deposition rate, Feq increased to a higher maximum with electronic cigarettes than with traditional cigarettes (Trassierra et al., 2015). Following the release of aerosols from electronic cigarettes, Feq values experienced a sustained increase over approximately three hours, accompanied by a particle number concentration 15 times higher than baseline measurements. During electronic cigarette use, the rise in the number concentration of particles in the air resulted in a decrease in the corresponding attachment mode to 24.4 ± 4.2 nm. After vaping, particle coagulation led to an increase in the mode to 86.6 nm (Trassierra et al., 2015). Alternatively, research conducted in the European Accredited Laboratory of Industrial Measurements found that over time, electronic cigarette use resulted in an activity size distribution of 120 - 165 nm (Fuoco et al., 2014). In another study conducted within a radon chamber, researchers observed distinct bimodal activity size distributions related to radon progeny in an environment with electronic cigarette-generated aerosols. The unattached clusters of radon progeny were found to exhibit activity at approximately 1 nm in diameter, with a nearly uniform size distribution. On the other hand, the attached progeny demonstrated an activity size distribution in the range of 100 – 400 nm, with this variation attributed to the number size distribution of electronic cigarette particles (Vaupotič 2024; Khalaf et al., 2019).

These results highlight the importance of time on both the number size distribution of particles produced by electronic cigarettes and the activity size distribution of radon progeny, emphasizing the need for subsequent investigation of the behavior of aerosols produced from these devices. Specifically, further research is needed to investigate the size distributions of particles emitted from electronic cigarettes during emission, over time, and under varying environmental conditions. As with traditional cigarettes, further research is needed to quantify the impact of electronic cigarettes in real-world scenarios before developing adjustment factors.

5.3.4 Candles

Various studies have investigated how candle burning influences indoor aerosol concentration, the unattached fraction, and $F_{\rm eq}$. Candle burning results in extremely high particle concentrations: 241,000 cm-3 (Afshari et al., 2005), 390,000 cm-3 (Huet et al., 2001), and 1,200,000 cm-3 (Vaupotič, 2011). However, candle burning primarily emits particles < 10 nm (Vaupotič, 2024). Specifically, research demonstrated that during candle burning, over 60% of particles were smaller than 10 nm and over 90% were smaller than 20 nm, resulting in total surface areas two to three times smaller than sources emitting larger particles (Vaupotič, 2011). The attachment rate is governed by the concentration of aerosols and the attachment

coefficient, which is a size-dependent variable (Porstendörfer, 1994), meaning that attachment with larger particles is preferred (Vaupotič, 2024). Because burning candles primarily releases small aerosols (nucleation mode), the attachment coefficient is smaller (Reineking et al., 1985). As shown in Table 5, most candle-burning experiments demonstrated an increase in F_{eq} due to elevated aerosol concentrations. However, despite high particle concentrations, the decrease in (f) and the increase in F_{eq} were smaller compared to sources that emit larger particles.

Further research found that during candle burning, the average attachment diameter decreased from 50 nm to approximately 15 nm. This decrease suggests that the particle emissions from the candle provided additional surfaces for progeny attachment. However, these smaller particles had faster deposition rates, causing the size distribution of progeny to return to background conditions within an hour. This indicates that progeny attached to the particles from candle burning deposited quickly, resulting in a reduced impact on the F_{eq} (Li & Hopke, 1992). Although this study presents a slightly different explanation for why candle burning results in a high number concentration but a relatively small impact on F_{eq} , it ultimately emphasizes that the faster deposition rates of smaller particles limit the long-term effect of candle burning on F_{eq} .

5.3.5 Cooking

The impact of cooking on F_{eq} cannot be generalized, as different cooking methods result in varying size distributions of particles (Li & Hopke, 1991). One study determined that cooking resulted in a high particle number concentration (250,000 cm⁻³) yet emitted particles in the nucleation mode, resulting in a F_{eq} comparable to the upper bound value of the background aerosol concentration (5000 cm⁻³) (Huet et al., 2001). Upon examining various cooking methods, frying food resulted in higher number-weighted and activity-weighted diameters and exhibited a greater attachment rate per hour compared to cooking soup, despite having a lower particle number concentration (Tu & Knutson, 1988). After frying steak, the particle concentrations in the kitchen and master bedroom were 250,000 cm⁻³ and 30,000 cm⁻³, respectively, and an increase in the number of attached particles and the F_{eq} occurred in both rooms (Li & Hopke, 1991). Frying steak emitted larger particles (accumulation mode), which led to an increase in the number of particles in the attached mode. The size distributions of the decay products remained high for longer periods than for vacuuming and candle burning, resulting in the observed increase in the F_{eq} after frying steak (Li & Hopke, 1991; Li & Hopke, 1992). Further research is necessary to comprehensively investigate the properties of aerosol sources such as cooking, vacuuming, and burning incense, including their number size distributions, attachment rates, and number concentrations.

Table 5. Aerosol sources and resulting F_{eq} values

0	Baseline		Result	o/ Dicc	D. C	
Source	Comment	Feq	Comment	Feq	% Difference	Reference
-	Clean air	0.3	Aerosols	0.8	166.7%	Wicke, 1981
-	Low aerosols	0.1 - 0.2	Increased aerosols	0.8 - 0.9	-	Mostafa et al., 2020
	EPA value	0.4	Urban	0.40	0%	Elals at al. 2010
-	EPA value	0.4	Rural	0.32	-0.20%	Jílek et al., 2010
			Park/playground	0.13	-43.5%	
	Average Rn-222	0.23	Building	0.23	0%	
C			Road/worksite	0.33	43.5%	V4 -1 1000
Surrounding area			Park/playground	0.017	-40.7%	Yu et al., 1999
	Average Rn-220	0.0287	Building	0.029	1.2%	
			Road/worksite	0.040	39.5%	
	Reported value from 1980- 1990	0.48	Beijing (urban and suburban)	0.58 ± 0.13	-	
PM _{2.5}			Xicheng (urban)	0.60 ± 0.16	-	H4 -1 2015
PIVI2.5			Changping (suburban)	0.57 ± 0.10	-	Hou et al., 2015
			Windows Open	0.69	43.75%	
Smoking	Before smoking	0.35 ± 0.03	After smoking	0.72 ± 0.06	-	Jasaitis & Girgždys, 2013
Smoking	Smoke free	0.40 ± 0.07	Smoke bearing	0.49 ± 0.08	-	Khan et al., 2012
C 1:	All houses	0.408	0 1 1 '	0.401	17.9%	II 1 4 1 1005
Smoking	Smoke free	0.383	Smoke bearing	0.481	25.6%	Hopke et al., 1995
Smoking	Blank	0.229 ± 0.036	After smoking	0.65 ± 0.021	-	Chu & Liu, 1996
Smoking	Without sources	0.34 ± 0.011	After smoking	0.52	52.9%	El-Hussein, 1996
Smoking	Before smoking	0.309 ± 0.01	After smoking	0.381 ± 0.0087	-	Trassierra et al., 2015
Smoking	Before smoking	0.36	After smoking	0.60	66.7%	Vaupotič, 2024
	Before smoking, room 1	0.31	After smoking	0.46	48.4%	
Smoking	Before smoking, room 9	0.42	After smoking	0.67	59.5%	Reineking & Porstendörfer, 1990
	Before smoking, room 10	0.26	After smoking	0.55	111.5%	1 015001101101, 1770

Table 5. Aerosol sources and resulting F_{eq} values (continued)

C.	Baseline		Result		o/ Dicc	D. C	
Source	Comment	Feq	Comment	Feq	% Difference	Reference	
			During smoldering	0.407	33.0%		
Cigarette smoldering (closed door)	Background	0.306	After 60 minutes	0.597	95.1%	Li & Hopke, 1991	
door)			After 135 minutes	0.549	79.4%		
Cigar	Before cigar	0.16	After cigar	0.56	250%	Huet et al., 2001	
	Before vaping, trial 1	0.233 ± 0.0111	After vaping	0.2945 ± 0.0036	-		
Vaping	Before vaping, trial 2	0.1695 ± 0.0088	After vaping	0.2026 ± 0.0009	-	Trassierra et al., 2015	
	Before vaping, trial 3	0.173 ± 0.0105	After vaping	0.2483 ± 0.001	-		
Candle	Without sources	0.34 ± 0.011	After candle	0.37	8.8%	El-Hussein, 1996	
	Before candle, room 1	0.31	After candle	0.34	9.7%		
Candle	Before candle, room 7	0.25	After candle	0.27	8.0%	Reineking & Porstendörfer, 1990	
	Before candle, room 10	0.26	After candle	0.31	19.2%	1 orstendorrer, 1990	
	Background	0.321	During burning	0.380	18.4%		
Candle (closed door)			After 55 minutes	0.401	24.9%	Li & Hopke, 1991	
			After 130 minutes	0.381	18.7%		
Candle	Before candle	0.31	After candle	0.41	32.3%	Vaupotič, 2024	
Incense	Blank	0.229 ± 0.036	After incense	0.745 ± 0.020	-	Chu & Liu 1996	
Mosquito Coils	Blank	0.229 ± 0.036	After mosquito coil	0.665 ± 0.022	-	Chu & Liu 1996	
			Vacuuming	0.389	-18.8%		
	Background Trial 1	0.479	After 60 minutes	0.340	-29.0%		
Vacuuming (closed door)			After 135 minutes	0.302	-37.0%	Li & Hopke, 1991	
vacuuming (closed door)			Vacuuming	0.263	11.4%	LI & Порке, 1991	
	Background Trial 2	0.236	After 60 minutes	0.348	47.5%		
			After 135 minutes	0.277	17.4%		
			Cooking	0.515	10.6%		
Cooking (kitchen)	Background	0.465	After 60 minutes	0.636	36.8%	Li & Hopke, 1991	
			After 135 minutes	0.693	48.9%		

6. BUILDING-SPECIFIC CHARACTERISTICS

6.1 AIR CLEANING METHODS

While primary methods for enhancing indoor air quality involve source identification and ventilation improvement, air cleaning systems serve as a beneficial supplementary approach (US EPA, 2023c). Specifically, effective strategies in addressing indoor radon progeny reduction include preventing radon gas infiltration, diluting radon and its progeny via ventilation systems, and employing air cleaning systems (Li & Hopke, 1992). Air cleaners, also referred to as air purifiers/air filters, are designed to improve indoor air quality by removing pollutants and particles from the air (US EPA, 2023c). Research has explored the impact of various air cleaning technologies on lowering the F_{eq}. Results from one study demonstrated that before activating an air purifier, the concentration of attached radon daughters was significantly higher than that of unattached daughters. In three repeated measurements, the concentrations of both attached and unattached radon decay products significantly decreased after the air purifier was turned on (Yanchao et al., 2021).

Research evaluating the impact of a HEPA (high-efficiency particulate air) filter on radon and thoron activity concentrations and effective dose (Wang et al., 2011) showed a decrease in aerosol concentration in the investigated room from 2000 cm⁻³ to 600 cm⁻³ at a filtration rate of 0.5 h⁻¹. For radon and thoron decay products, this filtration rate resulted in a reduced PAEC of 10% and 12%, respectively. At this same filtration rate, the concentration of unattached decay products increased by 120% for radon and 400% for thoron (Wang et al., 2011). Overall, filtration rates of 0.2 h⁻¹ and above substantially decreased concentrations and inhalation doses of thoron decay products, while the reduction in inhalation dose was less pronounced for radon decay products (Wang et al., 2011).

The fractional collection efficiency of a mechanical filter varies with particle diameter. For particles in the range of 10–100 nm, diffusion dominates due to Brownian motion. In the 100–1000 nm range, both diffusion and interception contribute to particle capture, while for particles larger than 1000 nm, inertial impaction and interception are the primary mechanisms of filtration (NIOSH, 2003). HEPA filters must capture at least 99.97% of particles at the most penetrating particle size (300 nm) and are more efficient at capturing particles larger or smaller than this size (US EPA, 2024b). Particle size should be noted in assessing the impact of HEPA filters on radon and thoron activity.

6.1.1 Comparisons of Cleaning Methods

Activating a HEPA filter resulted in a rapid decrease in particle concentration indoors (Rajala et al., 1985). In a Slovenian kindergarten, running a mobile air cleaner for several hours at a flow rate of 700 – 1200 m³ h⁻¹ in a closed room significantly reduced aerosol particle concentration larger than 30 nm from 4300 cm⁻³ to 300 cm⁻³ and increased the unattached fraction from 0.09 to 0.48 (Vaupotiĕ, 2017). These unattached daughters, with higher diffusion coefficients and deposition rates than attached radon daughters, deposited more quickly on room surfaces, decreasing the Feq. The use of a fan and an electrostatic precipitator also reduced both aerosol concentration and the total activity of airborne radon daughters. However, it remains unclear whether this reduction was due to enhanced deposition on the chamber surfaces or plate-out on the fan (Rajala et al., 1985). Nevertheless, these air cleaning systems effectively reduced the Feq by lowering particle concentration. In particle-free air, HEPA filters were also effective in reducing the activity of unattached radon daughters (Rajala et al., 1985). In a dwelling in Okinawa, Japan, the use of an air purifier equipped with both HEPA and activated carbon filters resulted in a significant reduction in Feq and a 174% increase in the unattached fraction. As a result, the air purifier achieved a 50% reduction in the effective dose from radon progeny (Kranrod et al., 2009). Additionally, the mobile air cleaner reduced the effective dose by a factor of approximately 3 (Vaupotiĕ, 2017). Effective dose is calculated for the entire body and

represents the sum of equivalent doses to all organs, adjusted based on the sensitivity of each organ to radiation (IRCP, 2019).

In a study conducted at a hospital in Taiwan, turning off a dehumidifier led to increased radon gas, radon progeny, and aerosol concentrations within three hours (Chen et al., 1998). The differences in F_{eq} with and without the dehumidifier are detailed in Table 6. Furthermore, the study examined 20 urban dwellings across Kaohsiung, Taiwan, and found a lower overall average radon concentration than observed at the hospital under both dehumidifier conditions. Although indoor radon gas concentration (IRC) does not correlate with F_{eq} , IRC remains a crucial factor for investigation. Interestingly, despite higher radon levels in the hospital, the F_{eq} was lower when the dehumidifier was operational compared to urban dwellings (F_{eq} = 0.49) (Chen et al., 1998).

Further research evaluated the effectiveness of three air purification systems in mitigating radon exposure (radiation levels in an area) and dose (radiation absorbed by individuals) (US EPA, 2024c; Hopke et al.,1993). These systems included a NO-RAD cleaner, which integrates ionization, filtration, and air circulation; an Electric Air Cleaner (EAC) equipped with a fan; and the Pureflow Air Treatment System, which consists of a multi-stage filtration setup with a flexible foam pre-filter, three activated carbon filters, and a HEPA filter (Li & Hopke, 1992; Hopke et al., 1993). The Pureflow system at high speeds was the most effective method for reducing exposure to progeny at elevated radon concentrations. The EAC also proved effective at reducing exposure but under lower exposure conditions (Hopke et al., 1993). Regarding dose, only the upper bound values from the NO-RAD trials exceeded those observed without a cleaning system. This was attributed to the NO-RAD exhibiting a lower removal efficiency for radon decay products, leading to a peak in the average activity-weighted size distribution between 1.5 and 5.0 nm (Hopke et al., 1993). Due to the increased dose-to-exposure ratio for this particle size, even a minor fraction of this activity can contribute significantly to the dose (Mohamed et al., 2008; Hopke et al., 1993). Additionally, the unattached fraction increased with the EAC and Pureflow (high-flow speed), whereas the NO-RAD ultimately reduced the unattached fraction (defined as 0.5 - 1.5 nm in this study). This discrepancy was hypothesized to result from the NO-RAD's uniform removal efficiency across the entire range of activity sizes, whereas the EAC and Pureflow systems were more effective at particle removal (Hopke et al., 1993). The existing literature explores various air cleaning systems configured at different settings for aerosol and progeny removal. Future studies should focus on evaluating the efficiency of additional air cleaning systems to identify the most effective types and optimal settings for reducing F_{eq} under diverse conditions. Moreover, new versions of purifiers, particularly the effective low-cost units (e.g., Corsi-Rosenthal Box), should be considered in the evaluation of the impact of cleaning devices on radon exposure.

6.1.2 Pureflow Air Treatment System

Two studies conducted a year apart examined the impact of aerosol sources on F_{eq} . Importantly, one employed the Pureflow Air Treatment System (Li & Hopke, 1992) while the other did not (Li & Hopke, 1991). The results showed that the Pureflow Air Treatment System reduced the F_{eq} regardless of the presence of additional aerosol sources such as candle burning, cigarette smoking, and vacuuming. The effectiveness of the air cleaner in reducing F_{eq} can be explained by examining aerosol concentration, attachment rates, average attachment diameter, and deposition rates.

When the air cleaning system was operational and additional aerosol sources were absent, particle concentration decreased from approximately $10,000 \text{ cm}^{-3}$ to $6,000 - 7,000 \text{ cm}^{-3}$. Subsequently, the attachment rate dropped from 4 h^{-1} to 2 h^{-1} , and the average attachment diameter decreased from 30 nm to 24 nm compared to the background conditions without the air filtration system. Additionally, the deposition rate of the unattached fraction increased from 3 h^{-1} to 7 h^{-1} . The air cleaning system effectively removed existing background particles from the room, thereby lowering the F_{eq} , as detailed in Table 6 (Li & Hopke, 1992). Integrating information about particle size distribution would provide a more comprehensive

understanding of the removal of background particles in the room. However, there was significant uncertainty associated with the size distribution of the background particles.

During candle burning, particle concentration increased but declined more rapidly with the air filter operating (Li & Hopke, 1991; Li & Hopke, 1992). For cigarette smoke, without the filtration system, the particle concentration increased to $100,000 \text{ cm}^{-3}$, and attachment rates reached 100 h^{-1} . Attachment rates increased during smoking and remained high even 135 minutes after smoking ceased. Thus, without the air cleaner, cigarette smoke particles persisted longer and significantly altered the activity-weighted size distributions of radon progeny (Li & Hopke, 1991). While the air cleaner was operating, the attached activity increased from 20% to 80% during smoking but returned to the background state after an hour, indicating the success of the air cleaner in removing particles from the air (Li & Hopke, 1992). With the air cleaner operating, the maximum F_{eq} values during smoking and candle burning were lower than the EPA assumed value and the F_{eq} values reported without the filter, demonstrating the effectiveness of the air cleaner at lowering F_{eq} values in the presence of various aerosol sources (Li & Hopke, 1992). Additionally, despite variations in aerosol concentration and particle size distribution observed in each vacuuming trial, the F_{eq} values were consistently higher without the cleaner compared to when the cleaner was operational. Regardless of the uncertainties in aerosol characteristics induced by vacuuming, the air cleaner effectively reduced the F_{eq} (Li & Hopke, 1991; Li & Hopke, 1992).

6.2 VENTILATION SYSTEMS

F_{eq} values are very much influenced by ventilation and the air exchange rate (air changes per hour (ACH)) within a given volume. A computational method in MATLAB was developed to determine the impact of ACH on F_{eq}. As ACH increased, F_{eq} decreased for both Rn-222 and Rn-220 (ORNL, 2022). Additionally, although indoor radon concentration and F_{eq} do not correlate, all types of ventilation systems maintained indoor radon concentrations below the recommended limit of 100 Bq m⁻³ at an ACH of 1 h⁻¹. When the ACH decreased to 0.01 h⁻¹, the average indoor radon concentrations in some areas exceeded the regulatory limit (Lee et al., 2016). Other research showed that in airtight buildings, pressure differences were enhanced by mechanical ventilation, which led to increased radon gas concentrations entering the indoor environment (Arvela et al., 2013).

Air conditioning (AC) serves as a form of mechanical ventilation commonly used indoors. To assess the effects of AC operation on F_{eq} values in an auditorium setting, measurements were conducted under two conditions: with AC turned off (AC OFF) and with AC activated (AC ON) (Kozak et al., 2013). The average radon concentration was 20 Bq m⁻³ for AC OFF compared to 15 Bq m⁻³ for AC ON. Interestingly, particle number concentrations remained consistent between both scenarios at 4.2×10^6 cm⁻³, while the particle mass concentration was higher when AC was off. The F_{eq} was lower with AC ON compared to AC OFF, as shown in Table 6 (Kozak et al., 2013).

While air conditioning was found to decrease the F_{eq} compared to non-air-conditioned environments, upon analysis of cooling systems, air-conditioned sites exhibited the lowest exchange of indoor and outdoor air, while electric fan sites demonstrated the highest. In these studies, windows were kept closed during air conditioning tests and were opened when utilizing electric fans and natural ventilation (Yu et al., 1996; Yu et al., 1999). The accumulation of Rn-222, Rn-220, and their progeny is expected to be more pronounced in areas characterized by reduced air exchange (Yu et al., 1999). Consequently, the average Potential Alpha Energy Concentration (PAEC) at air-conditioned sites was higher than that of naturally ventilated sites, which in turn exceeded that of sites with electric fans (Yu et al., 1996; Yu et al., 1999). Additionally, in environments with less ventilation, higher concentrations of aerosol particles facilitate greater attachment of radon progeny. Ventilation also decreases the F_{eq} by enhancing the probability of progeny depositing onto indoor surfaces (Yu et al., 1996). As a result of these factors, electric fan sites had the smallest F_{eq} , whereas air-conditioned sites had the largest. In a tamper study, the F_{eq} decreased by an average of 34.3%

following the operation of a 20-inch electric fan during seven separate tests. Detailed findings are summarized in Table 6 (Brodhead, 1994).

6.3 ACTIVE AND INACTIVE HOURS

Two studies were conducted in Slovenian elementary and secondary schools. The first measured the F_{eq} in 13 kindergartens from early January to mid-March 2000. Approximately 75% of the kindergartens had a lower F_{eq} during working hours compared to the entire 24-hour continuous monitoring period (Vaupotič & Kobal, 2001). This could potentially be attributed to the intermittent ventilation commonly used in schools, where the ventilation rate is higher during school hours. The second study focused on F_{eq} in predominantly single-story buildings without air conditioning. Due to student movement and the opening of doors and windows, the plate-out of aerosols was higher during working hours, leading to a reduction in aerosol concentration and lower F_{eq} values (El-Hussein, 1996; Vaupotič & Kobal, 2006). A study examining office buildings in Tokyo, Japan, found that the average annual F_{eq} values were higher during 24-hour measurements than during working hours. This discrepancy was attributed to the automatic operation of air conditioning during working hours (9:00 am - 5:00 pm, Monday to Friday) (Tokonami et al., 2003).

6.4 STRUCTURAL FEATURES

Structural features, including building material, wall coverings, and floor level, primarily affect indoor radon concentration (IRC) rather than F_{eq} . As a result, there is limited data regarding F_{eq} and these factors. Moreover, IRC does not always correlate with the F_{eq} . Despite this distinction, IRC is important in inhalation dose (Kandari et al., 2016), and factors influencing IRC will therefore be briefly discussed here in addition to F_{eq} .

Results from a nationwide study on radon exposure in 2,093 United Kingdom (UK) residences were analyzed to determine the percentage of variation in IRC attributable to various factors, including building materials (wall and floor), double glazing (double-pane windows), and floor level (Gunby et al., 1993). Double glazing, building materials, floor type, and floor level of the living area accounted for 1.7%, 1.1%, 0.4%, and 1.4%, respectively, of the total variation between indoor radon concentration levels across the UK.

6.4.1 Energy Efficiency Measures

Thermal retrofitting involves implementing measures to enhance the thermal performance of a building, thereby improving energy efficiency by allowing the building to heat quickly and retain heat for longer periods (Recart & Dossick, 2022). Across 3,400 dwellings in France, IRC was an average of 21% higher in homes with thermal retrofitting compared to those without. This increase could be due to reduced air permeability and the inconsistent implementation of ventilation post-retrofitting (Collignan et al., 2016). In kindergartens in the Czech Republic, renovations of older buildings to improve their energy efficiency resulted in increased airtightness and, subsequently, an increased IRC (Fojtikova & Rovenska, 2014). Similarly, an observational study on energy efficiency and IRC found that energy-efficient measures elevated indoor radon levels. Specifically, homes equipped with double glazing, loft insulation, and wall insulation showed notably higher radon levels, with a geometric mean that was 79% greater compared to homes without retrofitting history (Symonds et al., 2019). Other findings indicated that although the IRC increased by 4-8 times following thermal retrofitting in some dwellings, the average rise in radon concentration due to these measures was not statistically significant (Yang et al., 2019).

6.4.2 Building Materials

Theoretical analysis conducted in rural dwellings in China found that mud and cave houses exhibited a smaller aerosol number size distribution, a higher unattached fraction, and a lower F_{eq} compared to brick houses. Their models suggested that the F_{eq} was higher in brick dwellings due to the larger aerosol size distribution rather than differences in emanation from the material (Li et al., 2011).

Compared to foundation type, construction period, window type, ventilation system type, and thermal retrofitting, building materials had the highest impact on indoor radon concentration (Collignan et al., 2016). Homes constructed using granite or other stone materials exhibited a 67% increase in IRC compared to those built with concrete and brick. Radon activity concentrations were the highest in granite, followed by sand, cement, brick, and sandstone. However, these materials exhibited radon exhalation rates below the ICRP limit (Hameed et al., 2014). Notably, one study found that floor type was the second most significant factor affecting changes in indoor radon concentration. In workrooms with different floor materials, the average IRC was 327 Bq m⁻³ for parquet, 227 Bq m⁻³ for ceramic tiles, 146 Bq m⁻³ for vinyl, and 71 Bq m⁻³ for laminate (Gulan et al., 2022).

6.4.3 Wall Coverings

Different types of covering materials demonstrated varying abilities to reduce the release of radon from concrete surfaces. Both paint and plastic-lined wallpaper effectively limited Rn-222 exhalation compared to plaster. However, only wallpaper showed effectiveness in reducing Rn-220 exhalation, while the reduction observed with paint was not statistically significant (Yu et al., 1999). A nationwide study of dwellings in India revealed that the differences in Rn-222 gas concentrations among various floor types were minimal or insignificant when the walls were plastered and painted. This indicates that in the studied dwelling, the majority of Rn-222 emanated from the walls, and that painting the walls reduced emanation (Ramachandan & Sathish, 2011). It is important to note that emanation predominantly impacts radon gas concentration, which does not always correlate with progeny activity or F_{eq} (Omori et al., 2016).

6.4.4 Floor Level

The investigation of IRC on different floor levels in residential buildings in Irbid, Jordan, yielded average values (Bq m⁻³) of 36.13, 27.85, 21.24, 15.83, and 12.86, for basement, first, second, third, and fourth floors, respectively (Al-Omari, 2015). Throughout 158 homes in Iowa, the yearlong basement and first-floor measurements of IRC (Bq m⁻³) were 181 and 104, respectively (Barros et al., 2016). As the primary source of indoor radon is the ground beneath the building (Vaupotič, 2024; Jasaitis & Girgždys, 2013), decreasing indoor concentrations of radon gas with increasing floor levels is logical. However, a study employing hierarchical modeling to analyze indoor radon concentrations due to various geological and building factors revealed that while basements and ground floors typically exhibited higher indoor radon levels compared to higher floors, the relationship was non-linear. Specifically, the decline in IRC with increasing floor level plateaued after the first floor and above (Borgoni et al., 2014).

Table 6. Building-specific characteristics and associated $F_{\text{eq}}\ values$

V. All.	Baseline		Result	%	D.C.		
Variable	Comment F _{eq}		Comment	Feq	Difference	Reference	
HEPA filter	Without	Without 0.80 Aft		0.10	-87.5%	Rajala et al., 1985	
Mobile air cleaner (pre and electrostatic filter)	Without	0.60	With	0.10	-83.3%	Vaupotic 2017	
Pureflow Air Treatment System, *	Door closed, no cleaner	0.3 – 0.5	Door closed, cleaner on	0.141	-	Li & Hanks 1002	
background aerosol concentration	Door opened, no cleaner	0.50	Door opened, cleaner on	0.23	-54%	Li & Hopke, 1992	
	Candle burning, no cleaner	0.380	Candle burning, cleaner on	0.187	-50.8%	Li & Hopke 1992; Li & Hopke 1991	
Pureflow Air Treatment System, candle burning (closed door, cleaner on for 7 hours)	55 minutes after	0.401	55 minutes after	0.177	-55.9%		
ourning (closed door, cleaner on for 7 hours	130 minutes after	0.381	130 minutes after	0.207	-45.7%	•	
Pureflow Air Treatment System, cigarette	Smoking, no cleaner	0.407	Smoking, cleaner on	0.304	-25.3%		
smoldering (closed door, cleaner on for 4	60 minutes after	0.597	60 minutes after	0.193	-67.7%	Li & Hopke 1992; Li & Hopke 1991	
hours)	135 minutes after	0.549	135 minutes after	0.208	-62.1%	Li & Hopke 1991	
	Vacuuming, no cleaner	0.326	Vacuuming, cleaner on	0.126	-61.3%		
Pureflow Air Treatment System, vacuuming (closed door, cleaner on for 9.5 hours)	60 minutes after	0.344	60 minutes after	0.115	-66.6%	Li & Hopke 1992; Li & Hopke, 1991	
(crossed door, creamer on for 7.5 hears)	135 minutes after	0.265	135 minutes after	0.124	-53.2%	Er & Hopke, 1991	
Dehumidifier	Without	0.71 ± 0.25	With	0.11 ± 0.04	-	Chen et al., 1998	
Air purifier (HEPA and activated carbon filter)	Without	0.27	With	0.08	-71%	Kranrod et al., 2009	
			Air conditioning	0.22 ± 0.11	-		
Specific ventilation	Average of all ventilation types	0.2053	Electric fan	0.18 ± 0.11	-	Yu et al., 1996	
			Natural	0.22 ± 0.13	-		

Table 6. Building-specific characteristics and associated Feq values (continued)

V - 11	Baseline		Result	%	D. C		
Variable	Comment	F _{eq} Comment		Feq	Difference	Reference	
			Air conditioning	0.039	33.1%		
Specific ventilation (Rn-220)	Average of all ventilation types	0.029	Electric fan	0.028	-4.4%		
	J. J		Natural	0.021	-28.3%	V 4 1 1000	
			Air conditioning	0.32	35.2%	Yu et al., 1999	
Specific ventilation	Average of all ventilation types	0.2367	Electric fan	0.22	-7.1%		
	J.F.		Natural	0.17	-28.2%		
		0.543	Medium speed	0.318	-41%		
Electric Fan	Before	0.25	High speed	0.20	-20%	Brodhead, 1994	
		0.48	Low speed, HVAC fan	0.233	-51%		
Air conditioning	AC OFF	0.61	AC ON	0.49	-19.7%	Kozak et al. 2013	
Active hours	Whole day	0.51	School hours (6:00 am - 4:00 pm)	0.38	-25.5%	Vaupotič & Kobal, 2001	
Active hours	Whole day	0.59	School hours (7:00 am – 2:00 pm)	0.47	-20.3%	Vaupotič & Kobal, 2006	
	Whole day (office A)	0.57	Working hours (9:00 am – 5:00 pm)	0.48	-15.8%		
Active hours	Whole day (office B)	0.41	Working hours (9:00 am – 5:00 pm)	0.39	-4.9%	Tokonami et al., 2003	
			Plaster	0.034	14.6%		
Wall coverings (Rn-220)	Average	0.0297	Paint	0.027	-9.0%		
			Wallpaper	0.028	-5.6%	1	
			Plaster	0.27	12.5%	Yu et al., 1999	
Wall coverings	Average	0.24	Paint	-	-		
			Wallpaper	0.23	-4.2%		
			Brick house	0.493	42.075		
House type	Average	0.347	Mud house	0.250	-27.954	Li et al., 2011	
			Cave house	0.297	-14.409		

^{*} Pureflow Air Treatment System: a multi-stage filtering system with 5 separate filters: a flexible foam pre-filter, three activated carbon filters, and a HEPA filter (Li & Hopke, 1992).

7. ENVIRONMENTAL AND METEOROLOGICAL CONDITIONS

7.1 RELATIVE HUMIDITY

 F_{eq} was found to increase with rising relative humidity (RH), though the rate of increase diminished above 70% RH (Chu & Liu, 1996). Some studies have suggested that this trend occurs because radon decay products attach to the tiny water droplets suspended in the air (Rabi & Oufni, 2018). Others have attributed it to the increased attachment of radon daughters to aerosols, which occurs as aerosol particle size grows with increasing humidity (Chu & Liu, 1996). The larger particle sizes and higher attachment rates resulted in an increased F_{eq} . Furthermore, humidity significantly impacted the deposition velocity of the unattached progeny, which decreased as RH rose, indicating a reduced diffusion coefficient at higher relative humidity levels. As the deposition velocity of unattached radon daughters decreased with increasing RH, F_{eq} increased (Chu & Liu, 1996). Measurements across three locations in India demonstrated an increase in F_{eq} and a decrease in (f) with rising humidity (Saini et al., 2017). Contrary to these findings, another study reported decreased F_{eq} values with increased relative humidity, as shown in Table 7. This study categorized RH into two groups: above and below 79% (Yu et al., 1999).

An additional research study measured the variation in F_{eq} in response to changes in RH during showering. Increased RH because of showering led to increased aerosol particle concentrations and an increased F_{eq} , as the process of aerosol attachment outpaced the deposition of unattached particles on surfaces (Rabi et al., 2021). This information may be particularly relevant for testing conditions during or immediately after a person showers and requires further exploration.

7.2 TEMPERATURE AND SEASONAL VARIATION

Radon and thoron F_{eq} values tend to be the lowest during the warmer, summer months and the highest during the colder, winter months (Jasaitis & Girgždys, 2013; Prasad et al., 2023; Ramola et al., 2016; Xie et al., 2015). Furthermore, the highest dose of radon progeny was observed during the winter (Mostafa et al., 2015). This can be explained largely by the increase in ventilation during summer. Conversely, ventilation is typically poor in the winter, due to closed doors and windows (Mostafa et al., 2015; Ramola et al., 2003; Ramola et al., 2016; Rey et al., 2022; Saini et al., 2017). In Canada, observed F_{eq} values were significantly higher than the EPA's assumed average (0.40), likely due to the colder climate and extensive use of heating and cooling systems, leading to more forced than natural ventilation (Chen & Marro, 2011). Conversely, in India, where average city temperatures exceed 20°C, the mean F_{eq} value was 0.36, which is below the EPA's assumed average (Chen & Harley, 2018). However, attempts to establish a direct relationship between regional average temperature and F_{eq} have revealed no significant correlations, highlighting the complexity of F_{eq} and its dependence on multiple factors that vary across nations and regions. Interestingly, the unattached fraction across three locations in India was highest in winter and lowest in summer, indicating the influence of multiple factors on both (f) and F_{eq} (Saini et al., 2017).

Although IRC does not correlate with F_{eq} , it is important to note that occupant behaviors, such as heating in winter and higher ventilation in the summer, significantly impact IRC. In winter, heating units create a warmer indoor environment compared to the colder and denser outdoor air. This results in warm air rising and escaping, causing cold air to be drawn in from below, pulling radon from beneath the house into the living space (US EPA, 2001). Moreover, temperature affects the formation of aerosols both indoors and outdoors (Thomsen et al., 2024; Kerminen et al., 2018), which influences the partitioning of radon.

7.3 PRECIPITATION AND BAROMETRIC PRESSURE

The average indoor F_{eq} during rainy days (> 0.04 mm day⁻¹) was lower than during dry days (< 0.04 mm day⁻¹). This difference was attributed to the reduced aerosol concentration during rainfall (i.e. wet

deposition), resulting in a higher amount of unattached Rn-222 progeny and a lower F_{eq} (Yu et al., 1999). In another investigation, most of the activity observed was in the accumulation mode. Following rainfall, a decrease in accumulation mode particles occurred, while there was no significant change in the concentration of nucleation mode particles. This suggests that accumulation mode particles are more susceptible to washout during rainfall (Mostafa et al., 2011).

Research regarding the impact of precipitation on Feq is limited. In contrast, more studies focus on how precipitation affects indoor radon concentration (IRC). While IRC does not correlate with Feq, it is still a significant parameter for evaluating radon exposure. One study showed that rainfall resulted in higher concentrations of Rn-222 gas entering homes due to the increased differences in barometric pressure between indoor and outdoor environments. Specifically, rainfall caused a decrease in barometric pressure inside the investigated basement, creating a higher pressure in the ground relative to the indoor environment. This pressure differential drove radon gas upward from the soil and inside the dwelling (Acree, 2014). Further research identified positive correlations between IRC and both outdoor barometric pressure and the difference in barometric pressure between indoor and outdoor environments. However, indoor barometric pressure alone showed no clear correlation with IRC (Xie et al., 2015). Analysis of several hundred homes in Virginia, United States, revealed that increased rainfall or snowfall enhanced the horizontal movement of soil radon gas, facilitating its entry into homes (Mose et al., 1991). In contrast, regression analysis showed that rainfall and barometric pressure had a relatively minor impact on variations in IRC (Rowe et al., 2022). These varying results highlight the complexity of precipitation's impact on indoor radon concentration (IRC), underscoring the need to consider cross-correlations with other environmental conditions and site-specific factors.

7.4 GEOLOGICAL AND TOPOGRAPHIC FACTORS

Similarly to variables like building materials and floor level, many geological factors such as rock type and proximity to faults are rarely studied in terms of impact on F_{eq} but have important implications concerning IRC. The interaction between soil permeability and radon concentrations in soil and rock significantly influences indoor radon levels, highlighting the impact of regional geology on indoor radon concentrations (Peake, 1988). Soil radon potential is an index reflecting soil gas concentration and soil permeability. Across Canada, the percentage of homes with IRC above the Canadian guideline of 200 Bq m⁻³ increased with higher soil radon potential (Chen & Ford, 2017).

The rock type around specific dwellings explained 5.9% of the IRC variation across homes in the UK (Gunby et al., 1993). In Poland, the greatest mean annual indoor radon concentrations occurred in areas where igneous and metamorphic rocks were at the surface (Przylibski et al., 2011). Another study discovered that homes constructed on carbonate bedrock exhibited IRC values that were, on average, 103.6 Bq m⁻³ higher than for homes built on siliclastic rock (Hahn et al., 2023). An Italian study recorded the percentage of indoor radon concentrations that were above 200 Bq m⁻³ for 11 different geological classes (types). The highest percentages were observed over dolomite rocks (30%), acid rocks (29%), and debris (33%). The lowest percentages occurred over alluvial plains (2%) and basic rocks (6%) (Borgoni et al., 2011). Moreover, elevated indoor radon levels were found in residences located on volcanic terrain (Vaupotič, 2024). Another study conducted a multiple regression analysis on 330 dwellings in Slovenia and found an elevated IRC among buildings constructed on limestone (Popit & Vaupotič, 2002).

In both Michigan and Minnesota, United States, higher altitudes were observed to correlate with increased IRC. However, it is important to note that the relationship between elevation and radon levels is complex and may not be solely attributed to altitude itself. Other factors such as soil permeability and varying geological compositions at different elevations could also contribute significantly to indoor radon levels (Carrion-Matta et al., 2021).

In the Garhwal Himalayas, high soil gas concentrations of radon were detected along the Main Boundary Thrust (MBT), a tectonically active area. Furthermore, a positive correlation was observed between soilgas radon levels and indoor radon concentrations in dwellings near the MBT (Kandari et al., 2016). According to other studies, the influence of soil radon on IRC was only significant when the soil gas radon concentration exceeded 20 kBq m-³. Below this value, there was no observed correlation between radon concentrations in soil gas and indoor environments (Vaupotič, 2024).

Geological faults near dwellings enhance the risk of elevated IRC by facilitating pathways for radon to migrate from the underlying bedrock to the surface (Drolet & Martel, 2015). In Canada, 22.8% of homes within 150 meters of a geological fault, and 15.2% of homes situated 150 – 700 meters from a fault, exceeded the Canadian IRC guideline of 200 Bq m-3. Restricting the analysis to dwellings situated on uranium-rich bedrock units revealed higher percentages: 30.7% and 17.5% for distances less than 150 meters and between 150 and 700 meters, respectively (Drolet & Martel, 2015). In the United States, residences in fault zones had a 41% greater likelihood of exceeding the US indoor radon action level (148 Bq m-3). Interestingly, homes equipped with crawlspaces exhibited an 85% reduction in the risk of exceeding the action level, suggesting that crawlspaces could be a protective factor for dwellings constructed in fault zones (Dai et al., 2019).

Table 7. Environmental conditions and resulting F_{eq} values

	Baseline F _{eq}		Result	o/ Dies	D. C		
Variable	Comment	Feq	Comment	Feq	% Difference	Reference	
Seasonal variation	Long term average of 18 Canadian cities	0.71	Summer average of 18 Canadian cities	0.65	-8.4%	Chen & Marro, 2011; Chen & Harley, 2018	
			Spring	0.49	3.7%	Jasaitis &	
	A viama a a	0.4725	Summer	0.43	-9.0%	Girgždys, 2011;	
Seasonal variation	Average	0.4723	Autumn	0.45	-4.8%	Jasaitis &	
			Winter	0.52	10.1%	Girgždys, 2013	
Seasonal variation (Rn-222)			Summer	0.24	-14.3%		
	Average	0.20	Winter	0.34	21.4%]	
		0.28	Autumn	0.29	3.6%	Ramola et al., 2003	
			Rainy	0.25	-10.7%		
	Average	0.09	Summer	0.05	-44.4%		
C 1 : (D 220)			Winter	0.16	77.8%		
Seasonal variation (Rn-220)			Autumn	0.09	0%		
			Rainy	0.06	-33.3%		
			Summer	0.5 ± 0.3	-		
Seasonal variation (Rn-222)	Average	0.63	Winter	0.8 ± 0.4	-	D 1 . 1 2022	
			Rainy	0.6 ± 0.3	-		
			Summer	0.01 ± 0.002	-	Prasad et al., 2023	
Seasonal variation (Rn-220)	Average	0.02	Winter	0.03 ± 0.002	-		
			Rainy	0.02 ± 0.01	-		
Second variation (Dr. 222)	Avanaga	0.43	Summer	0.41	-5.6%		
Seasonal variation (Rn-222)	Average	0.43	Winter	0.46	5.1%	Soini et al. 2017	
Second variation (Dr. 220)	Avanaga	0.031	Summer	0.028	-11.7%	Saini et al., 2017	
Seasonal variation (Rn-220)	Average	0.031	Winter	0.035	11.7%		
Average temperature	EPA assumed value	0.40	India (T > 20°C)	0.36	-10%	Chen & Harley, 2018	

Table 7. Environmental conditions and resulting F_{eq} values (continued)

77 • 11	Baseline F _{eq}		Result	Result							
Variable —	Comment	Feq	Comment	Feq	% Difference	Reference					
			25 °C	0.51	8.5%						
Water temperature	2000	0.45	30 °C	0.53	12.8%	D 11 . 1 2021					
(showering)	20°C	0.47	35 °C	0.54	14.9%	Rabi et al., 2021					
			40 °C	0.56	19.1%						
			30%	0.25	-28.6%						
			40%	0.32	-8.6%						
D 1 (' 1 '1')		0.25	50%	0.36	2.9%	D 1: 4 1 2010					
Relative humidity	Average	0.35	60%	0.38	8.6%	Rabi et al., 2018					
			70%	0.40	14.3%						
			80%	0.42	20.0%						
			30%	0.147 ± 0.22	-						
	Average		40%	0.342 ± 0.031	-						
			50%	0.552 ± 0.030	-						
Relative humidity		Average	Average	Average	Average	Average	0.559	60%	0.695 ± 0.018	-	Chu & Liu, 1996
			70%	0.705 ± 0.030	-						
			80%	0.740 ± 0.026	-						
			90%	0.732 ± 0.042	-						
			50%	0.46	9.5%						
			60%	0.47	11.9%						
Relative humidity (showering)	40% RH	0.42	70%	0.51	21.4%	Rabi et al., 2021					
			80%	0.59	40.5%						
			90%	0.65	54.8%						
Relative humidity (Rn-222)	< 79% RH	0.31 ± 0.13	0.31 ± 0.13 > 79% RH 0.15 ± 0.07		-	Vn et el 1000					
Relative humidity (Rn-220)	<79% RH	0.038 ± 0.015	> 79% RH	0.019 ± 0.008	-	Yu et al., 1999					
Rainfall (Rn-222)	< 0.04 mm day ⁻¹	0.32	> 0.04 mm day-1	0.15	-51.3%	Vu et al. 1000					
Rainfall (Rn-220)	< 0.04 mm day ⁻¹	0.039	> 0.04 mm day ⁻¹	0.019	-51.3%	Yu et al., 1999					

8. DISCUSSION

 F_{eq} is a unitless measurement that represents the disequilibrium between radon and its progeny. F_{eq} is crucial for conversions from pCi to working level (WL), a standard metric used to assess radon exposure. Additionally, the F_{eq} plays a vital role in understanding the actual exposure to radon decay products, which are the primary contributors to lung cancer risk from radon. The derived F_{eq} value for residential dwellings in the RVISL calculator is set at 0.89, which serves as an overprotective value for the screening tool, relying solely on ACH simulations. This conservative estimate ensures a margin of safety, minimizing the risk of underestimating radon exposure. However, it also underscores the need for a more nuanced approach that accounts for the various factors influencing F_{eq} . The RVISL calculator currently allows for user input and adjustment regarding the air exchange rate. However, various parameters besides ACH have been shown to affect the F_{eq} and are not available for adjustment in the RVISL calculator. These include aerosol concentration and composition indoors (whether from outdoor PM2.5 or indoor sources such as smoking or candle burning), specific building characteristics (type of ventilation and presence of air cleaners), and environmental conditions (relative humidity, precipitation, and seasonal variation). Additionally, factors that impact indoor radon concentration are briefly explained. Indoor radon concentration, while relevant to dose considerations, has not been found to correlate directly with F_{eq} .

8.1 SUMMARY OF THE IMPACT OF AEROSOLS, AIR CLEANING, AND ENVIRONMENTAL CONDITIONS

Aerosols, or solids/liquids suspended in air, significantly influence the F_{eq} because radon progeny attaches to these particles. The attachment process depends on both the size-dependent attachment coefficient and the aerosol concentration within the indoor environment. Increased indoor aerosol concentrations from outdoor $PM_{2.5}$ reduce the unattached fraction, creating a positive correlation between $PM_{2.5}$ levels and indoor F_{eq} values. Smoking cigarettes increases the concentration of aerosols in the accumulation mode indoors, leading to a corresponding rise in F_{eq} . Conversely, the positive correlation between candle burning and F_{eq} is less pronounced, despite the high aerosol concentrations produced, because these aerosols exist primarily in nucleation mode. These impacts are depicted in Figure 2.

Air cleaning systems demonstrated effectiveness in reducing F_{eq} by decreasing the activity concentration of attached and, in some cases, unattached progeny. Analysis of specific ventilation systems revealed that air conditioning (AC) lowered the F_{eq} relative to conditions without AC. However, when compared to the use of electric fans and natural ventilation (open windows), AC exhibited the highest F_{eq} . This finding underscores the importance of air exchange rates in managing indoor radon. Structural features of buildings were examined, though the results primarily pertained to variations in indoor radon concentration.

Environmental conditions (meteorological and geological) were also investigated, with geological factors relating mainly to indoor radon concentration. It was generally observed that the F_{eq} increased with rising relative humidity, although the rate of increase diminished as RH approached 70% and above. However, results were not consistent across all studies, showcasing the complicated relationships between various factors influencing F_{eq} . With seasonal and temporal variation, the highest F_{eq} values were observed in the winter seasons and lowest in the summer. This was attributed mainly to the fact that increased ventilation occurs in the summer. Additionally, trends of regional average temperature and F_{eq} were not identified, again showcasing the complexity of F_{eq} and the importance of analyzing the interacting and independent factors that modify it.

High Aerosols - Higher F_{eq}

Low Aerosols - Lower F



Figure 2 The variation of F_{eq} based on varying mass loading of indoor air aerosols produced (e.g. cooking, candle lighting, and smoking) and removed (e.g., air purifier) by different indoor events.

8.2 FUTURE APPLICATIONS TO RVISL CALCULATOR

This research aims to offer real-world data and insights on factors influencing F_{eq} that could enhance the accuracy and applicability of the RVISL calculator. Understanding the multifactorial nature of the F_{eq} and its impact on the conversion to WL is crucial for accurate radon exposure assessment and effective public health interventions. Ultimately, this paper demonstrates that the studied factors significantly modify the F_{eq} , illustrating the importance of incorporating adjustment factors and laying a foundation for further research.

Currently, the US EPA's RVISL calculator utilizes models that do not address the comparative effects of smoking versus non-smoking (US EPA, 2011). Based on the results compiled in this review, smoking increases the bronchial dose, overall excess lifetime cancer risk, and F_{eq} (see Figure 3). A modification to the RVISL calculator to account for the impacts of smoking on the F_{eq} should be considered. However, most existing studies on cigarette smoke have been conducted in controlled chamber environments, where variables are isolated. Chamber studies should be continued, as they are invaluable for understanding the mechanisms of interaction between radon progeny and aerosols. Nevertheless, it is important to recognize that chamber studies do not replicate the complexity of real-world settings. In actual environments, fluctuating humidity, temperature changes, and the presence of multiple aerosol sources introduce variability. This means that data from chamber studies may not directly apply to diverse scenarios, emphasizing the need for real-world data to validate findings and ensure the accuracy of adjustment factors across all settings. Additionally, research is needed to quantify the impact of cigarette smoking on F_{eq} based on the number of cigarettes smoked per day. This will help in the development of adjustment factors that represent real smoking scenarios.

Incorporating air quality data from a representative sample of cities could refine the calculator's handling of outdoor pollution impacts. Smog and other anthropogenic emissions increase aerosol concentrations, affecting the attachment and behavior of radon progeny in indoor environments. Existing evidence suggests that smog significantly impacts F_{eq} and that considering regional air quality variations would yield more accurate assessments of radon exposure risks, especially in areas with high smog levels. Although early

data suggests that adjustment factors for smog would be beneficial, the existing research is insufficient to develop them at this time. More research is needed to quantify the impact of smog and $PM_{2.5}$ on F_{eq} across different regions and environmental conditions, as current studies are limited to cities in Japan and China. Additionally, the impact of outdoor $PM_{2.5}$ on indoor air quality is influenced by a variety of environmental and building-specific factors, which warrants further investigation. As more data is gathered, the RVISL calculator can be updated.

Air cleaning systems consistently reduced the F_{eq} (as seen in Figure 4), presenting an opportunity for the development of an adjustment factor. Specifics regarding the need for additional research on air cleaning systems will be addressed in Section 8.3.2. Additionally, further research is needed to determine whether the effects of environmental and building-specific factors on F_{eq} arise from individual variables or interactions among multiple factors, as current data is inconsistent. As our understanding of these factors improves, modifications to the RVISL calculator should be considered to enhance its effectiveness in risk assessment and mitigation.

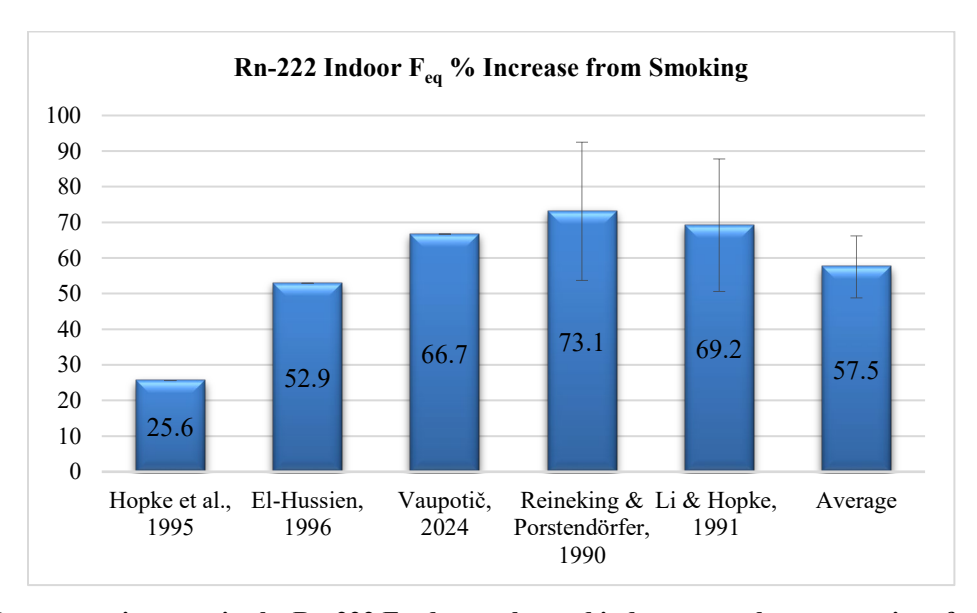


Figure 3. Percentage increase in the Rn-222 Feq due to elevated indoor aerosol concentrations from smoking

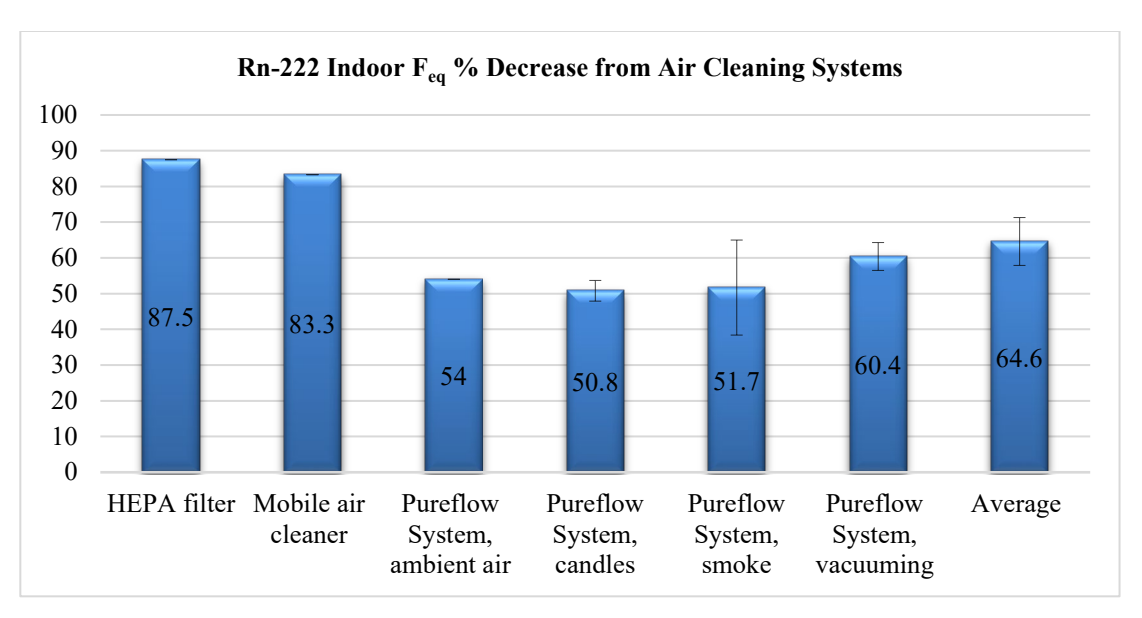


Figure 4. Percentage decrease in the Rn-222 Feq due to the presence of air-cleaning systems

8.3 FUTURE RESEARCH

Many variables besides ACH can have a significant impact on F_{eq} . However, further studies are essential before accurate adjustment factors can be developed. F_{eq} is affected by a multitude of interacting variables, including aerosol concentration, particle size distribution, humidity, temperature, and ventilation. These factors interact in non-linear and sometimes unexpected ways, making it challenging to fully understand their impact without sophisticated analysis. For example, high humidity can enhance particle size through condensation, which when combined with aerosol sources like cigarette smoke, may significantly increase the F_{eq} . Conversely, factors such as effective ventilation can mitigate the effects of cigarette smoke. Analyzing the F_{eq} requires the consideration of various factors simultaneously and in isolation. This complexity makes it challenging to pinpoint specific trends or predict outcomes under different scenarios, emphasizing the difficulties in developing accurate adjustment factors based on current research alone.

It is well established that indoor radon concentrations are influenced by a complex interplay of geological, environmental, meteorological, and site-specific variables. Subsequently, a variety of analytical techniques determine how these factors contribute to variations in indoor radon concentration across different sites. In one study, researchers used chi-square tests, bivariate correlation coefficient analysis, and logistic regression models to explore the relationships between indoor radon concentrations and various housing and geological characteristics (Dai et al., 2019). Additionally, mixed effect models (hierarchical models) were employed to assess how measurable factors account for variability in indoor radon concentrations. These models provided insights into the relative impact of site-specific, geological, and environmental conditions on indoor radon concentration (Borgoni et al., 2014). Advanced analytical techniques quantify the strength and nature of relationships among variables, providing a comprehensive understanding of how specific factors influence indoor radon levels and enabling the dissection of complex interactions. To gain a clearer understanding of how various factors interact and impact F_{eq}, studies using similar analytical methods are needed. Additionally, more extensive research is required to explore factors that influence the F_{eq} of Rn-220 and Rn-219.

8.3.1 Aerosols

Further research is required in several specific areas to establish accurate adjustment factors for aerosols in the context of F_{eq} . First, a deeper understanding of how various aerosol sources interact is important.

Laboratory-based research using controlled chambers should continue to investigate aerosol behavior in the presence of radon progeny, with a focus on how multiple aerosol sources affect both number and activity size distribution. Aerosols generated from simultaneous activities, like cigarette smoking and cooking, may differ significantly in number size distribution compared to those produced from each activity individually, potentially impacting F_{eq} . Investigating how these sources interact and affect aerosol behavior, including attachment rates and the partitioning between unattached and attached forms, is crucial. Multiphase aerosol dynamic models could simulate the effects of multiple aerosol sources under varying conditions and integrate radon decay product attachment. Sensitivity analysis will help identify the most significant factors influencing F_{eq} , while predictive modeling and machine learning techniques could further refine our understanding and application of these factors. Techniques such as principal component, multivariate, and regression analysis can lead to an enhanced understanding.

Results from laboratory and theoretical studies will provide valuable insights for developing field measurement protocols and are essential for accurately interpreting field data (Vaupotič, 2024). Real-world experiments should be conducted under varying environmental conditions to assess how different factors impact aerosol behavior. This includes utilizing real-time monitoring of particle size distribution and aerosol interactions. Field studies can validate the findings of theoretical and laboratory-based experiments, which can then inform the development of accurate adjustment factors. Additionally, field experiments are essential for quantifying aerosol exposure based on real-world behaviors, such as the number of cigarettes smoked per day or the duration for lit candles. It is also imperative to address the interaction of radon with the chemical components of the particles. These studies will help determine how the presence of various aerosol sources impacts F_{eq} in actual living environments, providing the data needed to develop adjustment factors for the RVISL calculator.

8.3.2 Air Cleaning Systems

Additional research is needed to comprehensively understand how air cleaning systems affect F_{eq} and to optimize their performance under various conditions. Controlled laboratory experiments and field studies should be designed to test air cleaning systems in real-world scenarios. This research is necessary for the development of accurate adjustment factors.

Research should focus on identifying the specific conditions under which the effectiveness of air cleaning systems fluctuates. This includes evaluating their effectiveness in diverse settings with different levels of temperature, humidity, aerosol concentrations, radon concentrations, and aerosol size distributions. It is important to determine if there are thresholds or limits beyond which these systems fail to maintain their efficiency in reducing the F_{eq} . Since air cleaning strategies demand energy consumption, an optimized system should be developed that accounts for energy usage while mitigating radon exposure.

Additionally, future studies should aim to identify which air cleaning systems are most effective across a broad range of applications. This involves comparing the performance of various filter types—such as HEPA filters, activated carbon filters, and electrostatic filters—in reducing radon progeny under different environmental conditions and in the presence of various aerosol sources. By identifying which air cleaning systems perform best in specific settings, researchers can offer more targeted recommendations for improving indoor air quality and reducing radon exposure. Efficiency curves should be developed to chart how well different air cleaning systems remove radon progeny across various conditions. Statistical analyses, including ANOVA and regression analysis, can help determine the significance of performance differences and identify the most effective systems for specific environments. Long-term evaluations are also crucial to understand the sustained effectiveness and durability of air cleaning systems. Results from these analyses and studies can identify optimal air cleaning systems, both in general and under specific environmental conditions, facilitating the development of adjustment factors.

8.3.3 Environmental and Building-Specific Characteristics

Given the limited and conflicting data regarding the impact of environmental factors on F_{eq} , further climate chamber experiments in controlled environments are essential. These tests allow for precise manipulation of variables such as humidity, temperature, and precipitation. This controlled approach can isolate and explain the impact of each variable on radon and thoron F_{eq} values. Furthermore, the impact of environmental and building-specific characteristics on aerosol sources requires further research. For instance, the extent to which outdoor $PM_{2.5}$ affects indoor air quality is influenced by various factors related to both the environment and building design (Hou et al., 2015). Understanding these interactions necessitates additional research to identify the conditions under which outdoor $PM_{2.5}$ concentrations are most likely to impact the F_{eq} .

As demonstrated in studies on IRC, it is possible to analyze both building-specific and environmental/ meteorological factors to identify which elements have the greatest impact on the variability of radon measurements across different dwellings. Subsequently, field studies utilizing multifactorial analysis techniques will be invaluable in exploring the complex interactions affecting F_{eq} . Bivariate correlation coefficient analysis can reveal relationships between continuous variables such as soil radon potential and humidity. Logistic regression models are useful for determining the likelihood of the modification of F_{eq} based on specific characteristics like the presence of a basement or geographic location. Hierarchical models will further enhance our understanding by assessing the influence of site-specific, geological, and environmental factors on variability in radon and thoron F_{eq} values. New methods such as machine learning and artificial intelligence techniques should also be utilized to provide better predictions of the F_{eq} based on several archived parameters that impact radon and thoron exposures. Longitudinal studies are necessary to analyze how F_{eq} fluctuates over time, accounting for seasonal changes and long-term trends. Overall, future research employing this multifaceted approach will yield deeper insights into how various factors interact and influence F_{eq} . This understanding will enable the development of adjustment factors tailored to the most relevant environmental and building-specific variables.

9. REFERENCES

- Acree, P. (2014). *The effect of rain and HVAC setting on radon levels in a home*. Riverwood International Charter School, Sandy Springs, Georgia, USA. https://aarst.org/proceedings/2014/2_-Acree_THE-EFFECT-OF-RAIN-AND-HVAC-SETTING.pdf.
- Afshari, A., Matson, U., & Ekberg, L.E. (2005). Characterization of indoor sources of fine and ultrafine particles: a study conducted in a full-scale chamber. *Indoor Air*, *15*, 141-150. https://doi:10.1111/j.1600-0668.2005.00332.x
- Al-Omari, S. (2015). Assessment of indoor radon levels and associated hazards: effects of floor levels in residential buildings. *International Journal of Low Radiation*, *9*, 5-6. https://www.inderscienceonline.com/doi/pdf/10.1504/IJLR.2014.068277
- Arvela, H., Holmgren, O., Raisbeck, H., & Vinha, J. (2013). Review of low-energy construction, air tightness, ventilation strategies and indoor radon: Results from Finnish houses and apartments. *Radiation Protection Dosimetry*, 162(3), 351-363. https://doi.org/10.1093/rpd/nct278
- Agency for Toxic Substances and Disease Registry (ATSDR). (2010). *Radon Toxicity*. https://www.atsdr.cdc.gov/csem/radon/radon.pdf
- Barros, N., Steck, D. J., & William Field, R. (2016). Utility of short-term basement screening radon measurements to predict year-long residential radon concentrations on upper floors. *Radiation Protection Dosimetry*, November 2016. https://doi.org/10.1093/rpd/ncv416
- Borgoni, R., Tritto, V., Bigliotto, C., & De Bartolo, D. (2011). A Geostatistical approach to assess the spatial association between indoor radon concentration, geological features and building characteristics: The case of Lombardy, northern Italy. *International Journal of Environmental Research and Public Health*, 8(5), 1420-1440. https://doi.org/10.3390/ijerph8051420
- Borgoni, R., De Francesco, D., De Bartolo, D., & Tzavidis, N. (2014). Hierarchical modeling of indoor radon concentration: How much do geology and building factors matter? *Journal of Environmental Radioactivity*, *138*, 227-237. https://doi.org/10.1016/j.jenvrad.2014.08.022
- Bossew, P. (2003). The radon emanation power of building materials, soils and rocks. *Applied Radiation and Isotopes*, *59*, 389-392. https://doi.org/10.1016/j.apradiso.2003.07.001
- Brodhead, B. (1994). *The effect of ventilation and filtration on radon decay product measurements*. WPB Enterprises. https://wpb-radon.com/pdf/RDP%20&%20Ventilation%20changes%2005.pdf
- Bundesamnt Für Strahlenschutz (BFS). (2024). *Radionuclides in Building Materials*. https://www.bfs.de/EN/topics/ion/environment/buildingmaterials/radionuclides/radionuclides node.html
- Carmona, R. H. (2005). National Health Advisory on Radon. Office of the Surgeon General. http://www.adph.org/radon/assets/surgeon_general_radon.pdf.
- Carrion-Matta, A., Lawrence, J., Kang, C., Wolfson, J. M., Li, L., Vieira, C. L., Schwartz, J., Demokritou, P., & Koutrakis, P. (2021). Predictors of indoor radon levels in the Midwest United States. *Journal of the Air & Waste Management Association*, 71(12), 1515-1528. https://doi.org/10.1080/10962247.2021.1950074
- Centers for Disease Control and Prevention (CDC). (2018). Dose Conversion Factors for Radon WLM, Revision 05. https://www.cdc.gov/niosh/ocas/pdfs/tibs/dc-t11-r5-508.pdf.
- Čeliković, I., Pantelić, G., Vukanac, I., Nikolić, J., Živanović, M., Cinelli, G., Gruber, V., Baumann, S., Quindos Poncela, L. S., & Rabago, D. (2022). Outdoor radon as a tool to estimate radon priority

- areas—A literature overview. *International Journal of Environmental Research and Public Health*, 19(2), 662. https://doi.org/10.3390/ijerph19020662
- Chen J., Liu, C.C., & Lin, Y.M. (1998). Measurement of equilibrium factor and unattached fraction of radon progeny in Kaohsiung, Taiwan. *Applied Radiation and Isotopes*, 49(12), 1613-1618. https://doi.org/10.1016/S0969-8043(98)00065-7
- Chen, J., Rahman, N.M., & Atiya, I.A. (2010). Radon exhalation from building materials for decorative use. *Journal of Environmental Radioactivity*, 101(4), 317-322. https://doi.org/10.1016/j.jenvrad.2010.01.005
- Chen, J., & Marro, L. (2011). Assessment of radon equilibrium factor from distribution parameters of simultaneous radon and radon progeny measurements. *Radiation and Environmental Biophysics*, 50(4), 597-601. https://doi.org/10.1007/s00411-011-0375-8
- Chen, J., & Ford, K. L. (2017). A study on the correlation between soil radon potential and average indoor radon potential in Canadian cities. *Journal of Environmental Radioactivity*, 166, 152-156. https://doi.org/10.1016/j.jenvrad.2016.01.018
- Chen, J., & Harley, N. H. (2018). A review of indoor and outdoor radon equilibrium factors part I: 222Rn. *Health Physics*, *115*(4), 490-499, https://doi.org/10.1097/hp.000000000000000909 and part II: 220Rn. *Health Physics*, *115*(4), 500-506, https://doi.org/10.1097/HP.00000000000000010.
- Cheng, J., Guo, Q., & Ren, T. (2012). Radon levels in China. *Journal of Nuclear Science and Technology*, 39(6), 695-699. https://doi.org/10.1080/18811248.2002.9715251
- Chu, T.C & Liu, H.L. (1996). Simulated equilibrium factor studies in radon chamber. *Applied Radiation and Isotopes*, 47(5-6), 543-550. https://doi.org/10.1016/0969-8043(95)00334-7
- Collé R.; Rubin, R. J.; Knab, L. I.; & Hutchinson, J. M. R. (1981). Radon transport through and exhalation from Building Materials: A review and assessment. Washington D.C., National Institute of Standards and Technology (NIST). https://nvlpubs.nist.gov/nistpubs/Legacy/TN/nbstechnicalnote1139.pdf
- Collignan, B., Le Ponner, E., & Mandin, C. (2016). Relationships between indoor radon concentrations, thermal retrofit and dwelling characteristics. *Journal of Environmental Radioactivity*, *165*, 124-130. https://doi.org/10.1016/j.jenvrad.2016.09.013
- Dai, D., Neal, F. B., Diem, J., Deocampo, D. M., Stauber, C., & Dignam, T. (2019). Confluent impact of housing and geology on indoor radon concentrations in Atlanta, Georgia, United States. Science of The Total Environment, 668, 500-511. https://doi.org/10.1016/j.scitotenv.2019.02.257
- Daniels, R.D., & Schubauer-Berigan, M.K. (2018). Radon in U.S. workplaces, a review. *Radiat Prot Dosimetry*, 176(3), 278-286. https://doi.org/10.1093/rpd/ncx007
- Darby, S., Hill, D., Auvinen, A., Barros-Dios, J. M., Baysson, H., Bochicchio, F., Deo, H., Falk, R., Forastiere, F., Hakama, M., Heid, I., Kreienbrock, L., Kreuzer, M., Lagarde, F., Mäkeläinen, I., Muirhead, C., Oberaigner, W., Pershagen, G., Ruano-Ravina, A., Ruosteenoja, E., Rosario, A.S., Tirmarche, M., Tomášek, L., Whitley, E., Wichmann, H.E., & Doll, R. (2005). Radon in homes and risk of lung cancer: Collaborative analysis of individual data from 13 European case-control studies. *BMJ*, 330(7485), 223. https://doi.org/10.1136/bmj.38308.477650.63
- Drolet, J.P., & Martel, R. (2015). Distance to faults as a proxy for radon gas concentrations in dwellings. *Journal of Environmental Radioactivity*, 152, 5-18. http://dx.doi.org/10.1016/j.jenvrad.2015.10.023
- El-Hussein, A. (1996). Unattached fractions, attachment and deposition rates of radon progeny in indoor air. *Applied Radiation and Isotopes*, 47(5-6), 515-523. https://doi.org/10.1016/0969-8043(96)00001-2

- European Environment and Health Information System (ENHIS) & World Health Organization (WHO). (2005). *Implementing Environment and Health Information System in Europe*. https://ec.europa.eu/health/ph/projects/2003/action1/docs/2003/1/28 frep en.pdf.
- Fojtikova, I., & Rovenska, K.N. (2014). Influence of some energy-saving measures on the radon concentration in some kindergartens in the Czech Republic. *Radiation Protection Dosimetry*, 160(1-3), 149-153. https://doi.org/10.1093/rpd/ncu073
- Fuoco, F.C., Buonanno, G., Stabile, L., & Vigo, P. (2014). Influential parameters on particle concentration and size distribution in the mainstream of e-cigarettes. *Environmental Pollution*, *184*, 523-529. https://doi.org/10.1016/j.envpol.2013.10.010
- Grundel, M. (2004). Differences between the activity size distributions of the different natural radionuclide aerosols in outdoor air. *Atmospheric Environment*. https://doi.org/10.1016/s1352-2310(04)00219-5
- Gulan, L., Stajic, J. M., Spasic, D., & Forkapic, S. (2022). Radon levels and indoor air quality after application of thermal retrofit measures—a case study. *Air Quality, Atmosphere & Health*, *16*(2), 363-373. https://doi.org/10.1007/s11869-022-01278-w
- Gunby, J.A., Darby, S.C., Miles, J.C.H., Green, B.M.R., & Cox, D.R. (1993). Factors affecting indoor radon concentrations in the United Kingdom. *Health Physics*, 64(1), 2-12. https://oce-ovid-com.libproxy.lib.unc.edu/article/00004032-199301000-00001/HTML
- Hahn, E. J., Haneberg, W. C., Stanifer, S. R., Rademacher, K., Backus, J., & Rayens, M. K. (2023). Geologic, seasonal, and atmospheric predictors of indoor home radon values. *Environmental Research: Health*, *I*(2), 025011. https://doi.org/10.1088/2752-5309/acdcb3
- Hameed, P., Pillai, G., Mazhar Nazeeb Khan, S., & Balasundar, S. (2014). Radon exhalation rate from the building materials of Tiruchirappalli district (Tamil Nadu state, India). *Radiation Protection and Environment*, *37*(3), 150. https://doi.org/10.4103/0972-0464.154869
- Harley, N.H., Chittaporn, P., Medora, R., & Merrill, R. (2010). Measurement of the indoor and outdoor 220Rn (thoron) equilibrium factor: application to lung dose. *Radiation Protection Dosimetry*, 141(4), 357-362. https://doi.org/10.1093/rpd/ncq228
- Health Canada. (2017). *Guide for Radon Measurements in Residential Dwellings*. https://www.canada.ca/content/dam/hc-sc/documents/services/publications/health-risks-safety/guide-radon-measurements-residential-dwellings/radon-measurements-homes-eng.pdf
- Hopke, P. K., Montassier, N., & Wasiolek, P. (1993). Evaluation of the effectiveness of several air cleaners for reducing the hazard from indoor radon progeny. *Aerosol Science and Technology*, *19*(3), 268-278. https://doi.org/10.1080/02786829308959635
- Hopke, P. K., Jensen, B., Li, C., Montassier, N., Wasiolek, P., Cavallo, A. J., Gatsby, K., Socolow, R. H., & James, A. C. (1995). Assessment of the exposure to and dose from radon decay products in normally occupied homes. *Environmental Science & Technology*, 29(5), 1359-1364. https://doi.org/10.1021/es00005a031
- Hopke, P. K. (1996). The initial atmospheric behavior of radon decay products. *Journal of Radioanalytical and Nuclear Chemistry Articles*, 203(2), 353-375. https://doi.org/10.1007/bf02041517
- Hou, C., Shang, B., Zhang, Q., Cui, H., Wu, Y., & Deng, J. (2015). Impact of haze-fog days to radon progeny equilibrium factor and discussion of related factors. *Radiation and Environmental Biophysics*, *54*(4), 475-480. https://doi.org/10.1007/s00411-015-0609-2

- Hu, J., Wu, Y., Saputra, M. A., Song, Y., Yang, G., & Tokonami, S. (2022). Radiation exposure due to 222Rn, 220Rn and their progenies in three metropolises in China and Japan with different air quality levels. *Journal of Environmental Radioactivity*, 244-245, 106830. https://doi.org/10.1016/j.jenvrad.2022.106830
- Huet, C., Tymen, G., & Bouland, D. (2001). Long-term measurements of equilibrium factor and unattached fraction of short-lived radon decay products in a dwelling comparison with Praddo Model. *Aerosol Science & Technology*, 35(1), 553-563. https://doi:10.1080/02786820117956
- Hussein, T., Hämeri, K., Heikkinen, M. S., & Kulmala, M. (2005). Indoor and outdoor particle size characterization at a family house in Espoo–Finland. *Atmospheric Environment*, *39*(20), 3697–3709. https://doi.org/10.1016/j.atmosenv.2005.03.011
- Hussein, T., Sogacheva, L., & Petäjä, T. (2018). Accumulation and coarse modes particle concentrations during dew formation and precipitation. *Aerosol and Air Quality Research*, 18(12), 2929-2938. https://doi.org/10.4209/aaqr.2017.10.0362
- International Atomic Energy Agency (IAEA). (n.d.). *Exposure to Radon*. https://www.iaea.org/sites/default/files/21/12/11_exposure_to_radon.pdf
- IAEA. (2021). What is Radon and How are We Exposed to It? https://www.iaea.org/newscenter/news/what-is-radon-and-how-are-we-exposed-to-it
- International Commission on Radiological Protection (ICRP). (2010). Lung cancer risk from radon and progeny and statement on radon. *IRCP Publication 115*, 40(1). https://doi.org/10.1016/j.icrp.2011.08.011
- ICRP. (2019). *Absorbed, Equivalent, and Effective Dose*. http://icrpaedia.org/Absorbed,_Equivalent,_and_Effective_Dose
- Jasaitis, D., & Girgždys, A. (2011). Influence of aerosol particle concentration on volumetric activities of indoor radon progeny. *Lithuanian Journal of Physics*, *51*(2), 155-161. https://doi.org/10.3952/lithjphys.51209
- Jasaitis, D., & Girgždys, A. (2013). The investigation of tobacco smoke influence on the changes of indoor radon and its short-lived decay products volumetric activities. *Journal of Environmental Engineering and Landscape Management*, 21(1), 59-66. https://doi.org/10.3846/16486897.2012.745415
- Jílek, K., Thomas, J., & Tomášek, L. (2010). First results of measurement of equilibrium factors F and unattached fractions f_p of radon progeny in Czech dwellings. *Nukleonika*, 55(4), 439-444. https://doi.org/10.1016/0969-8043(96)00001-2
- Kandari, T., Aswal, S., Prasad, M., Bourai, A.A., & Ramola, R.C. (2016). Estimation of annual effective dose from radon concentration along Main Boundary Thrust (MBT) in Garhwal Himalaya. *Journal of Radiation Research and Applied Sciences*, *9*(3), 228-233. https://doi.org/10.1016/j.jrras.2015.10.005
- Kardos, R., Gregorič, A., Jónás, J., Vaupotič, J., Kovács, T., & Ishimori, Y. (2015). Dependence of radon emanation of soil on lithology. *Journal of Radioanalytical and Nuclear Chemistry*, 304(3), 1321-1327. https://doi.org/10.1007/s10967-015-3954-3
- Keller, G., Hoffmann, B., & Feigenspan, T. (2001). Radon permeability and radon exhalation of building materials. *Science of The Total Environment*, 272(1-3), 85-89. https://doi.org/10.1016/s0048-9697(01)00669-6
- Kerminen, V.-M., Chen, X., Vakkari, V., Petäjä, T., Kulmala, M., & Bianchi, F. (2018). Atmospheric new particle formation and growth: review of field observations. *Environmental Research Letters*, *13*, *103003*, 10.1088/1748-9326/aadf3c.

- Khalaf, H.N., Mostafa, Y.A., & Zhukovsky, M. (2019). Effect of electronic cigarette (EC) aerosols on particle size distribution in indoor air and in a radon chamber. *Nukleonika*, *64(1)*, 31-38. https://doi:10.2478/nuka-2019-0004
- Khan, A.J., Prasad, R., & Tyagi, R.K. (1992). Measurement of radon exhalation rate from some building materials. *Nuclear Tracks Radiat. Meas.*, 20(4), 609-610.
- Khan, F., Ali, N., Khan, E. U., Khattak, N. U., Raja, I. A., Baloch, M. A., & Rajput, M. U. (2012). Study of indoor radon concentrations and associated health risks in the five districts of Hazara Division, Pakistan. *Journal of Environmental Monitoring*, *14*(11), 3015. https://doi.org/10.1039/c2em30445g
- Kolarž, P., Vaupotič, J., Kobal, I., Ujić, P., Stojanovska, Z., & Žunić, Z. S. (2017). Thoron, radon and air ions spatial distribution in indoor air. *Journal of Environmental Radioactivity*, 173, 70-74. https://doi.org/10.1016/j.jenvrad.2016.11.006
- Kozak, K., Grzadziel, D., Połednik, B., Mazur, J., Dudzińska, M. R., & Mroczek, M. (2013). Air conditioning impact on the dynamics of radon and its daughter's concentration. *Radiation Protection Dosimetry*, 162(4), 663-673. https://doi.org/10.1093/rpd/nct347
- Kranrod, C., Tokonami, S., Ishikawa, T., Sorimachi, A., Janik, M., Shingaki, R., Furukawa, M., Chanyotha, S., & Chankow, N. (2009). Mitigation of the effective dose of radon decay products through the use of an air cleaner in a dwelling in Okinawa, Japan. *Applied Radiation and Isotopes*, 67(6), 1127-1132. https://doi.org/10.1016/j.apradiso.2009.02.087
- Kranrod, C., Chanyotha, S., Tokonami, S., & Ishikawa, T. (2021). A simple technique for measuring the activity size distribution of radon and thoron progeny aerosols. *Journal of Environmental Radioactivity*, 229-230, 106506. https://doi.org/10.1016/j.jenvrad.2020.106506
- Lee, J. E., Park, H. C., Choi, H. S., Cho, S. Y., Jeong, T. Y., & Roh, S. C. (2016). A numerical study on the performance evaluation of ventilation systems for indoor radon reduction. *Korean Journal of Chemical Engineering*, 33(3), 782-794. https://doi.org/10.1007/s11814-015-0214-8
- Li, C.S., & Hopke, P. K. (1991). Characterization of radon decay products in a domestic environment. *Indoor Air*, *I*(4), 539-561. https://doi.org/10.1111/j.1600-0668.1991.00018.x
- Li, C.S., & Hopke, P.K. (1992). Air filtration and radon decay product mitigation. *Indoor Air 2*, 84-100. https://www.aivc.org/sites/default/files/airbase 6433.pdf
- Li, H., Zhang, L., & Guo, Q. (2011). Behaviours and influence factors of radon progeny in three typical dwellings. *Journal of Radiological Protection*, *31*(1), 135-140. https://doi.org/10.1088/0952-4746/31/1/010
- Mohamed, A., Ahmed, A., Ali, E., & Yuness, M. (2008). Attached and Unattached Activity Size Distribution of Short-Lived Radon Progeny (214Pb) and Evaluation of Deposition Fraction. Environmental Physics Conference, International Energy Agency. https://inis.iaea.org/collection/NCLCollectionStore/_Public/41/046/41046589.pdf
- Mohamed, A., El-hady, M.A., Moustafa, M., & Yuness, M. (2014). Deposition pattern of inhaled radon progeny size distribution in human lung. *Journal of Radiation Research and Applied Sciences*, 7(3), 333-337. https://doi.org/10.1016/j.jrras.2014.05.004
- Mose, D.G., Mushrush, G.W., & Chrosniak, C.E. (1991). Seasonal indoor radon variations related to precipitation. *Environmental and Molecular Mutagenesis*, 17(4), 223-230. https://doi.org/10.1002/em.2850170402
- Mostafa, A. M., Tamaki, K., Moriizumi, J., Yamazawa, H., & Iida, T. (2011). The weather dependence of particle size distribution of indoor radioactive aerosol associated with radon decay products. *Radiation Protection Dosimetry*, *146*(1-3), 19-22. https://doi.org/10.1093/rpd/ncr097

- Mostafa, A., Yamazawa, H., Uosif, M., & Moriizumi, J. (2015). Seasonal behavior of radon decay products in indoor air and resulting radiation dose to human respiratory tract. *Journal of Radiation Research and Applied Sciences*, 8(1), 142-147. https://doi.org/10.1016/j.jrras.2014.12.007
- Mostafa, Y.A., Khalaf, H.N.B., & Zhukovsky, M. (2020). Radon decay products equilibrium at different aerosol concentrations. *Applied Radiation and Isotopes*, *156*, 108981. https://doi.org/10.1016/j.apradiso.2019.108981
- National Nuclear Data Center (NNDC). (2020). *Q-Value Calculator (QCalc)*. https://www.nndc.bnl.gov/qcalc/
- National Research Council (US). (1999). Committee on Evaluation of US EPA Guidelines for Exposure to Naturally Occurring Radioactive Materials. Washington (DC): National Academies Press. https://www.ncbi.nlm.nih.gov/books/NBK230646/.
- National Institute for Occupational Safety and Health (NIOSH). (2003). Guidance for filtration and aircleaning systems to protect building environments from airborne chemical biological or radiological attacks. Department of Health and Human Services. https://www.cdc.gov/niosh/docs/2003-136/pdfs/2003-136.pdf?id=10.26616/NIOSHPUB2003136
- Nero, A. V.; Gadgil, A. J.; Nazaroff, W. W.; & Revzan, K. L. (1990). Indoor Radon and Decay Products: Concentrations, Causes, and Control Strategies. DOE: Office of Health and Environmental Research. https://www.osti.gov/servlets/purl/6318312.
- Nøjgaard, J. K., Nguyen, Q. T., Glasius, M., & Sørensen, L. L. (2012). Nucleation and Aitken mode atmospheric particles in relation to O3 and NOX at semirural background in Denmark. *Atmospheric Environment*, 49, 275 283. https://doi.org/10.1016/j.atmosenv.2011.11.040
- Occupational Safety and Health Administration (OSHA). (2021). *Radon*. https://www.osha.gov/chemicaldata/883
- Omori, Y., Prasad, G., Sorimachi, A., Sahoo, S. K., Ishikawa, T., Vidya Sagar, D., Ramola, R. C., & Tokonami, S. (2016). Long-term measurements of residential radon, thoron, and thoron progeny concentrations around the Chhatrapur placer deposit, a high background radiation area in Odisha, India. *Journal of Environmental Radioactivity*, *162-163*, 371-378. https://doi.org/10.1016/j.jenvrad.2016.06.009
- Oak Ridge National Laboratory (2022). Air Exchange Rate Impact on Activity Equilibrium Factors and Inhalation Fractional Equilibrium Factors for Rn, Xe, Kr, Ar, Ne, and Their Progeny in Vapor Intrusion, Risk, and Dose Models. Environmental Sciences Division.
- Paquet, F., Bailey, M.R., Leggett, R.W., Lipsztein, J., Marsh, J., Fell, T.P., Smith, T., Nosske, F., Eckerman, K.F., Berkovski, V., Blanchardon, E., Gregoratto, D., & Harrison, J.D. (2017). *Occupational Intakes of Radionuclides: Part 3*. IRCP Publication 137, ICRP 46. https://www.icrp.org/publication.asp?id=ICRP%20Publication%20137
- Peake, R.T. (1988). Radon and geology in the United States. *Radiation Protection Dosimetry*, 24(1-4), 173-178. https://doi.org/10.1093/oxfordjournals.rpd.a080265
- Phong Thu, H. N., Van Thang, N., & Hao, L. C. (2020). The effects of some soil characteristics on radon emanation and diffusion. *Journal of Environmental Radioactivity*, 216, 106189. https://doi.org/10.1016/j.jenvrad.2020.106189
- Popit, A., & Vaupotič, J. (2002). Indoor radon concentrations in relation to geology in Slovenia. *Environmental Geology*, 42(4), 330-337. https://doi.org/10.1007/s00254-002-0526-y
- Porstendörfer, J. (1994). Properties and behaviour of radon and thoron and their decay products in the air. *Journal of Aerosol Science*, 25(2), 219-263. https://doi.org/10.1016/0021-8502(94)90077-9

- Porstendörfer, J., & Reineking, A. (2000). *Radon Characteristics Related to Dose for Different Living Places of the Human*. International Radiation Protection Association, Isotope Laboratory for Biological and Medical Research. https://www.irpa.net/irpa10/cdrom/00109.pdf
- Porstendörfer, J. (2001). Physical parameters and dose factors of the radon and thoron decay products. *Radiation Protection Dosimetry*, *94*(4), 365-373. https://doi.org/10.1093/oxfordjournals.rpd.a006512
- Prasad, M., Bossew, P., Shetty, T., & Ramola, R. (2023). Characteristics of 222Rn and 220Rn equilibrium factors in the indoor environments. *Journal of Environmental Radioactivity*, 268-269, 107262. https://doi.org/10.1016/j.jenvrad.2023.107262
- Przylibski, T. A., Żebrowski, A., Karpińska, M., Kapała, J., Kozak, K., Mazur, J., Grządziel, D., Mamont-Cieśla, K., Stawarz, O., Kozłowska, B., Kłos, B., Dorda, J., Wysocka, M., Olszewski, J., & Dohojda, M. (2011). Mean annual 222Rn concentration in homes located in different geological regions of Poland first approach to whole country area. *Journal of Environmental Radioactivity*, 102(8), 735-741. https://doi.org/10.1016/j.jenvrad.2011.03.018
- Rabi, R., & Oufni, L. (2018). Evaluation of indoor radon equilibrium factor using CFD modeling and resulting annual effective dose. *Radiation Physics and Chemistry*, *145*, 213-221. https://doi.org/10.1016/j.radphyschem.2017.10.022
- Rabi, R., Oufni, L., Cheikh, K., Youssoufi, E., Badry, H., & Errami, Y. (2021). Modeling of radon and its short-lived decay products during showering: Dose to adult members of the public. *World Journal of Nuclear Science and Technology*, 11(02), 84-99. https://doi.org/10.4236/wjnst.2021.112006
- Rajala, M., Janka, K., Lehtimäki, M., Kulmala, V., Graeffe, G., & Keskinen, J. (1985). The control of radon progeny by air treatment devices. *Science of the Total Environment*, 45, 493-498. https://doi.org/10.1016/0048-9697(85)90254-2
- Ramachandan, T.V., & Sathish, L.A. (2011). Nationwide indoor ²²²Rn and ²²⁰Rn map for India: a review. *Journal of Environmental Radioactivity, 102(11)*, 975-986. https://doi.org/10.1016/j.jenvrad.2011.06.009
- Ramola, R. C., Negi, M. S., & Choubey, V. M. (2003). Measurement of equilibrium factor "F" between radon and its progeny and thoron and its progeny in the indoor atmosphere using nuclear track detectors. *Indoor and Built Environment*, 12(5), 351-355. https://doi.org/10.1177/142032603035368
- Ramola, R.C., Negi, M.S., & Choubey, V.M. (2005) Radon and thoron monitoring in the environment of Kumaun Himalayas: survey and outcomes. *Journal of Environmental Radioactivity*, 79(1), 85-92. https://doi.org/10.1016/j.jenvrad.2004.05.012
- Ramola, R. C., Prasad, M., Kandari, T., Pant, P., Bossew, P., Mishra, R., & Tokonami, S. (2016). Dose estimation derived from the exposure to radon, thoron and their progeny in the indoor environment. *Scientific Reports*, 6(1). https://doi.org/10.1038/srep31061
- Recart, C., & Dossick, C.S. (2022). Hygrothermal behavior of post-retrofit housing: a review of the impacts of energy efficiency upgrade strategies. *Energy & Buildings*, 262. https://doi.org/10.1016/j.enbuild.2022.112001
- Reineking, A., Becker, K.H., & Porstendörfer, J. (1985). Measurements of the unattached fractions of radon daughters in houses. *The Science of the Total Environment*, 45, 261-270. https://doi.org/10.1016/0048-9697(85)90227-X
- Reineking, A., & Porstendörfer, J. (1990). "Unattached" fraction of short-lived RN decay products in indoor and outdoor environments. *Health Physics*, 58(6), 715-727. https://doi.org/10.1097/00004032-199006000-00003

- Rey, J. F., Goyette, S., Gandolla, M., Palacios, M., Barazza, F., & Goyette Pernot, J. (2022). Long-term impacts of weather conditions on indoor radon concentration measurements in Switzerland. *Atmosphere*, *13*(1), 92. https://doi.org/10.3390/atmos13010092
- Rowe, J.E., Kelly, M., & Price, L.E. (2002). Weather system scale variation in radon-222 concentration of indoor air. *Science of the Total Environment*, 248(1-3), 157-166. https://doi.org/10.1016/S0048-9697(01)00876-2
- Saini, K., Singh, P., Singh, P., Bajwa, B., & Sahoo, B. (2017). Seasonal variability of equilibrium factor and unattached fractions of radon and thoron in different regions of Punjab, India. *Journal of Environmental Radioactivity*, *167*, 110-116. https://doi.org/10.1016/j.jenvrad.2016.11.022
- Seinfeld, J. H., & Pandis, S. N. (2016). Atmospheric chemistry and physics: From air pollution to climate change. John Wiley & Sons.
- Skubacz, K., & Wołoszczuk, K. (2019). Size distribution of ambient and radioactive aerosols formed by the short-lived radon progeny. *Journal of Sustainable Mining*, 18(2), 61-66. https://doi.org/10.1016/j.jsm.2019.03.006
- Soniya, S.R., Jojo, P.J., & Khandaker, M.U. (2023). Study of radium content and radon exhalation rates in raw building materials used in southern India. *Physics Open, 17*, 100169. https://doi.org/10.1016/j.physo.2023.100169
- Swedjemark, G.A. (1983). The equilibrium factor F. *Health Physics*, 45(2), 453-462). https://journals.lww.com/health-physics/abstract/1983/08000/the_equilibrium_factor_f.21.aspx
- Swedjemark, G. A., & Makitalo, A. (1990). Recent Swedish experiences in 222Rn control. *Health Physics*, *58*(4), 453-460. https://doi.org/10.1097/00004032-199004000-00007 Mohammed 2008, 90
- Symonds, P., Rees, D., Daraktchieva, Z., McColl, N., Bradley, J., Hamilton, I., & Davies, M. (2019). Home energy efficiency and radon: An observational study. *Indoor Air*, 29(5), 854-864. https://doi.org/10.1111/ina.12575
- Thomsen, D., Iversen, E. M., Skønager, J. T., Luo, Y., Li, L., Roldin, P., Priestley, M., Pedersen, H. B., Hallquist, M., Ehn, M., Bilde, M., & Glasius, M. (2024). The effect of temperature and relative humidity on secondary organic aerosol formation from ozonolysis of Δ3-carene. *Environmental Science: Atmospheres*, 4(88-103). https://doi.org/10.1039/D3EA00128H
- Tokonami, S., Furukawa, M., Shicchi, Y., Sanada, T., & Yamada, Y. (2003). Characteristics of radon and its progeny concentrations in air-conditioned office buildings in Tokyo. *Radiation Protection Dosimetry*, 106(1), 71-75. https://doi.org/10.1093/oxfordjournals.rpd.a006338
- Trassierra, C., Cardellini, F., Buonanno, G., & De Felice, P. (2015). On the interaction between radon progeny and particles generated by electronic and traditional cigarettes. *Atmospheric Environment*, *106*, 442-450. https://doi.org/10.1016/j.atmosenv.2014.06.017
- Tu, K.W., & Knutson, E.O. (1988). Indoor radon progeny particle size distribution measurements made with two different methods. *Radiation Protection Dosimetry*, 24(1-4), 251-255. https://doi.org/10.1093/oxfordjournals.rpd.a080280
- United Nations. Scientific Committee on the Effects of Atomic Radiation (UNSCEAR). (2000). Sources and effects of ionizing radiation: Sources.
- United States Environmental Protection Agency (US EPA). (2001). *Building Radon Out*. https://www.epa.gov/sites/default/files/2014-08/documents/buildradonout.pdf
- US EPA. (2011). US EPA Radiogenic Cancer Risk Models and Projections for the U.S. Population. Office of Radiation and Indoor Air, 402-R-11-001. Retrieved June 24, 2022, from https://www.epa.gov/sites/default/files/2015-05/documents/bbfinalversion.pdf.

- US EPA. (2014). Radiation Risk Assessment At CERCLA Sites: Q & A. Retrieved July 11, 2022, from https://semspub.epa.gov/work/HQ/176329.pdf.
- US EPA. (2016). A Citizen's Guide to Radon: The Guide to Protecting Yourself and Your Family from Radon. https://www.epa.gov/sites/default/files/2016-12/documents/2016 a citizens guide to radon.pdf.
- US EPA. (2023a). Radon Vapor Intrusion Screening Level Calculator User's Guide. https://epa-visl.ornl.gov/radionuclides/documents/RVISL%20User's%20Guide 20220106.pdf.
- US EPA. (2023b). Radon Vapor Intrusion Screening Level Calculator. https://epa-visl.ornl.gov/radionuclides/.
- US EPA (2023c). Air Cleaners and Air Filters in the Home. https://www.epa.gov/indoor-air-quality-iaq/air-cleaners-and-air-filters-home
- US EPA (2024a). *How does PM Affect Human Health?* https://www3.epa.gov/region1/airquality/pm-human-health.html
- US EPA. (2024b). What is a HEPA filter? https://www.epa.gov/indoor-air-quality-iaq/what-hepa-filter#:~:text=It%20is%20an%20acronym%20for,of%200.3%20microns%20(%C2%B5m)
- US EPA. (2024c). *About Exposure and Dose Rates*. https://www.epa.gov/radnet/about-exposure-and-dose-rates
- US EPA. (2024d). *Radon in Homes, Schools, and Buildings*. https://www.epa.gov/radtown/radon-homes-schools-and-buildings
- United States Federal Code of Regulations (US CFR). (2021). *Health and environmental protection standards for uranium and thorium mill tailings* (40 CFR 192.11). https://www.govinfo.gov/content/pkg/CFR-2021-title40-vol27/pdf/CFR-2021-title40-vol27-part192.pdf
- Vaupotič, J. & Kobal, I. (2001). Radon exposure in Slovene kindergartens based on continuous radon measurements. *Radiation Protection Dosimetry*, 95(4), 359–364. https://doi:10.1093/oxfordjournals.rpd.a0
- Vaupotič, J., & Kobal, I. (2006). Effective doses in schools based on nanosize radon progeny aerosols. *Atmospheric Environment*, 40(39), 7494-7507. https://doi.org/10.1016/j.atmosenv.2006.07.006
- Vaupotič, J. (2011). Nano particles including radon decay products in ambient air. *Chemistry, Emission Control, Radioactive Pollution and Indoor Air Quality*. https://doi:10.5772/16369
- Vaupotič, J. (2017). The effect of air filtration on the fraction of unattached radon products. *Radiation & Applications*, 2(2), 115-117. https://doi: 10.21175/RadJ.2017.02.024
- Vaupotič, J. (2024). Radon and its short-lived products in indoor air: Present status and perspectives. *Sustainability*, 16(6), 2424. https://doi.org/10.3390/su16062424
- Wang, J., Meisenberg, O., Chen, Y., Karg, E., & Tschiersch, J. (2011). Mitigation of radon and thoron decay products by filtration. *Science of The Total Environment*, 409(19), 3613-3619. https://doi.org/10.1016/j.scitotenv.2011.06.030
- Wasiolek, P.T., & James, A.C. (1995). Outdoor radon dose conversion coefficient in South-Western and South-Eastern United States. Radiation Protection Dosimetry, 59(4), 269-278. https://doi.org/10.1093/oxfordjournals.rpd.a082660

- Wicke, A. (1981). *Radon Daughter Equilibrium in Dwellings*. Second Special Symposium on natural Radiation Environment (136-139). https://inis.iaea.org/collection/NCLCollectionStore/ Public/12/618/12618345.pdf
- Williamson, C. J., Kupc, A., Rollins, A., Kazil, J., Froyd, K. D., Ray, E. A., Murphy, D. M., Schill, G. P., Peischl, J., Thompson, C., Bourgeois, I., Ryerson, T. B., Diskin, G. S., DiGangi, J. P., Blake, D. R., Bui, T. P., Dollner, M., Weinzierl, B., & Brock, C. A. (2021). Large hemispheric difference in nucleation mode aerosol concentrations in the lowermost stratosphere at mid- and high latitudes. *Atmospheric Chemistry and Physics*, 21(11), 9065-9088. https://doi.org/10.5194/acp-21-9065-2021
- World Health Organization (WHO). (2010). WHO guidelines for indoor air quality: selected pollutants. World Health Organization, Regional Office for Europe. https://apps.who.int/iris/handle/10665/260127.
- Xie, D., Liao, M., & Kearfott, K. J. (2015). Influence of environmental factors on indoor radon concentration levels in the basement and ground floor of a building A case study. *Radiation Measurements*, 82, 52-58. https://doi.org/10.1016/j.radmeas.2015.08.008
- Yanchao, S., Bing, S., Hongxing, C., & Yunyun, W. (2021). Study on the effect of air purifier for reducing indoor radon exposure. *Applied Radiation and Isotopes*, *173*, 109706. https://doi.org/10.1016/j.apradiso.2021.109706
- Yang, S., Pernot, J.G., Jörin, C.H., Niculita-Hirzel, H., Perret, V., & Lincina, D. (2019). Radon investigation in 650 energy efficient dwellings in Western Switzerland: impact of energy renovation and building characteristics. *Atmosphere*, 10(12), 777. https://doi.org/10.3390/atmos10120777
- Young, L., & Keeler, G. J. (2007). Summertime Ultrafine particles in urban and industrial air: Aitken and nucleation mode particle events. *Aerosol and Air Quality Research*, 7(3), 379-402. https://doi.org/10.4209/aaqr.2007.02.0012
- Yu, C., Sun, Y., & Wang, N. (2023). Outdoor radon and its progeny in relation to the particulate matter during different polluted weather in Beijing. *Atmosphere*, 14(7), 1132. https://doi.org/10.3390/atmos14071132
- Yu, K. N., Young, E. C., & Li, K. C. (1996). A study of factors affecting indoor radon properties. *Health Physics*, 71(2), 179-184. https://doi.org/10.1097/00004032-199608000-00008
- Yu, K., Cheung, T., Guan, Z., Young, E., Mui, B., & Wong, Y. (1999). Concentrations of 222Rn, 220Rn and their progeny in residences in Hong Kong. *Journal of Environmental Radioactivity*, 45(3), 291-308. https://doi.org/10.1016/s0265-931x(98)00114-3



APPENDIX A. OUTDOOR FEO

The International Atomic Energy Agency reported that because radon is significantly diluted outdoors, outdoor exposure poses little to no associated health risks (IAEA, 2021). Furthermore, ATSDR states that "background levels of radon in outdoor air are generally quite low and represent a goal for reducing indoor levels" (ATSDR, 2010). The United Nations Scientific Committee on the Effects of Atomic Radiation (UNSCEAR) found worldwide annual doses for indoor and outdoor radon inhalation of 0.41 and 0.07, respectively (UNSCEAR, 2000). Since doses from outdoor radon exposure are generally lower than those from indoor exposure, there are fewer surveys conducted on outdoor radon. However, outdoor radon measurements could serve to identify areas in need of remediation (Čeliković et al., 2022). Concentrations of radon outdoors are influenced by both exhalation rates in the area and atmospheric mixing as well as seasonal and temporal differences.

UNSCEAR determined that the global average outdoor F_{eq} is approximately 0.6, which is lower than the previously estimated value of 0.8 (UNSCEAR, 2000). A 2018 review found that the outdoor F_{eq} was higher for 10 out of 11 studies that measured both indoor and outdoor Rn-222 F_{eq} values, with an average difference of 40%. These differences were attributed to the fact that there are fewer surfaces available for progeny deposition outdoors than indoors (Chen & Harley, 2018). Table 8 presents the nationwide outdoor average F_{eq} value across China, with the national indoor average reported as 0.47 ± 0.10 . Other results indicated that the largest activity fraction of radon in outdoor air is found in the accumulation mode, yielding an (f) value of 0.63. Differences in results due to aerosol concentration and meteorological factors were not significant (Porstendörfer, 2001).

There is limited data regarding F_{eq} values for thoron (Rn-220) in outdoor air. Available information indicates that the F_{eq} of Rn-220 is 10 times lower in outdoor air compared to indoor environments (Chen & Harley, 2018; Harley et al., 2010). No data on outdoor F_{eq} values for actinon (Rn-219) are available.

Table 8. Outdoor Rn-220 and Rn-222 Feq values

$\begin{array}{c c} & & & & \\ \hline Parent & & & \\ \hline & Comment & & F_{eq} \\ \end{array}$			Additional Information	Reference
		Feq	Additional Information	Kelefelice
Rn-220	2-year period	0.005	The average outdoor concentration of Rn-220 was 15 Bq m ⁻³ over a four-year period	Harley et al., 2010
Rn-222	Average value	0.54 ± 0.13	Average value of various international sites	Chen & Harley, 2018
Rn-222	Average value	0.59 ± 0.12	Average value of sites throughout China	Cheng et al., 2012
Rn-222	Average Value	0.6	Global average	UNSCEAR, 2000
Rn-222	Average Value	0.63	Average of 16 locations in the United States	Wasiolek & James, 1995



APPENDIX B. EXHALATION AND EMANATION

The exhalation rate measures the amount of radon activity released into indoor or outdoor air from a surface over time (Porstendörfer, 1994). Various building materials and manufacturing processes result in different exhalation rates (Keller et al., 2001; Khan et al., 1992). However, soil exhalation rates are higher than those from building materials for both Rn-220 and Rn-222 (Porstendörfer, 1994). Radon exhalation from building materials typically does not significantly impact indoor radon levels. Exemptions include alum shale concrete and materials made from volcanic tuff, which have high radium concentrations (WHO, 2010; Keller et al., 2001). A study on interior home decoration materials available in the Canadian market revealed that granite slabs exhibited the highest radon exhalation rates. However, even if an entire floor were covered with granite at its maximum measured exhalation rate, it would only contribute 18 Bq m⁻³ to the indoor air of a tightly sealed house with an air change rate of 0.3 h⁻¹ (Chen et al., 2010). In Germany, the Federal Office for Radiation Protection (Bundesamt für Strahlenschutz (BFS)) determined that concrete, brick, porous concrete, and sand-lime brick were not typically the cause for increased indoor Rn-222 levels (BFS, 2024). On the other hand, recent studies have reported higher Rn-220 levels indoors, attributed to exhalation from thorium present in building materials (Vaupotič, 2024; Chen & Harley, 2018; Kolarž et al., 2017). Exhalation rates are shown in Table 9.

Emanation is the process by which radon is released from solid mineral grains into air-filled pores, with the emanation power (E) indicating the portion of radon that escapes into these pores. Emanation power encompasses recoil and diffusion, with recoil assumed to be the predominant factor because of the low diffusion coefficient of gases within solid materials (Porstendörfer, 1994). Emanation occurs in soil, rock, groundwater, and building materials (Porstendörfer, 1994; Vaupotič, 2024). Values for emanation power of Rn-220 and Rn-222 are shown in Table 10. The emanation power was shown to increase with moisture content and stabilize at a constant value, which was dependent on the range of grain sizes (Phong Thu et al., 2020). Very small increases in water content increased emanation rates. When soil humidity increased up to 10%, the emanation power increased. Once the humidity surpassed 10%, the emanation power reached a saturation point, and the strong positive correlation weakened (Bossew, 2003). Conversely, in both Michigan and Minnesota, United States, low soil moisture was associated with higher indoor radon concentrations (Carrion-Matta et al., 2021). Another report suggested that, although meteorological effects are important, the intrinsic properties of materials generally have a greater impact on emanation (Collé et al., 1981). Additionally, research demonstrated that areas near faults and carbonate formations exhibited the highest emanation fraction values (Kardos et al., 2015). Radon release from building materials is determined by the activity of Ra-226 and the intrinsic characteristics of the material (BSF, 2024). Values for Ra-226 concentrations in various materials are shown in Table 11.

Table 9. Surface exhalation rates of Rn-222 and Rn-220 from various mediums (mBq m⁻² s⁻¹)

Medium	Comment	Rn-222	Rn-220	Reference
Building materials	Typically (range)	0.5 (0.1 – 3)	50 (10 – 200)	Porstendörfer, 1994
Granite	Normalized on a 10-cm thickness	0.25	30	Keller et al., 2001
Granite	Average (range)	0.011 (0.007 – 0.019)	-	Soniya et al., 2023
Granite slabs	Average	4.86 e-4	-	Chen et al, 2010
Marble	-	0.011	-	Khan et al., 1992
Marble	Average (range)	0.008 (0.002 – 0.016)	-	Soniya et al., 2023
Slate slabs	Average	3.47 e-4	-	Chen et al, 2010
Brick	Average (range)	0.062 (0.029 – 0.088)	-	Soniya et al., 2023
Brick, solid type	-	4.81 e-5	-	Collé et al., 1981
Unfired clay bricks	-	0.047	-	Khan et al., 1992
Fired clay bricks	-	0.026	-	Khan et al., 1992
Brick	Normalized on a 10-cm thickness	0.05	10	Keller et al., 2001
Sandstone	Normalized on a 10-cm thickness	0.30	45	Keller et al., 2001
Vitrified tile	Average (range)	0.015 (0.005 – 0.028)	-	Soniya et al., 2023
Concrete	Normalized on a 10-cm thickness	0.30	20	Keller et al., 2001
Concrete	-	0.018	-	Khan et al., 1992
Ordinary concrete, unknown composition		3.48 e-4		
Ordinary concrete, gravel and sand	Average	3.16 e-4	-	Collé et al., 1981
Light weight concrete, clay based		5.55 e-5		
Cement	-	0.010	-	Khan et al., 1992
Soil	Typically (range)	20 (1 – 50)	1000	Porstendörfer, 1994

Table 10. Emanation power of Rn-222 and Rn-220 from various mediums (E)

Medium	Comment	Rn-222	Rn-220	Reference
Building materials	Typically (range)	0.05 (0.005 – 0.3)	$0.01 \; (0.002 - 0.06)$	Porstendörfer, 1994
Bricks	Median values	0.025	-	Bossew, 2003
Red brick	Mean	0.051		Collé, 1981
Silica brick	Mean	0.163	-	Colle, 1981
Ceramic tiles	Median values	0.006	-	Bossew, 2003
Stones	Median values	0.205	-	Bossew, 2003
Sand (quartz)	Median values	0.059	-	Bossew, 2003
Portland cement	Mean	0.041	-	Collé et al., 1981
Slag	Mean (range)	0.0070 (0.0024 – 0.0153)	-	Collé et al., 1981
Soil	Typically (range)	0.1 (0.01 – 0.5)	0.05 (0.01 - 0.2)	Porstendörfer, 1994
Soil	Mean (range)	0.289 (0.121 – 0.501)	-	Collé et al., 1981
Dry soil	Median values	0.19	-	Bossew, 2003

Table 11. Ra-226 concentration in various mediums (Bq kg⁻¹)

Medium	Comment	Ra-226	Reference
Red brick	M	20.0	C-114 -4 -1 1001
Silica brick	Mean	6.67	Collé et al., 1981
Brick, clinker brick	Mean (range)	50 (10 – 200)	BFS, 2024
Clay	Mean (range)	< 40 (< 20 – 90)	BFS, 2024
Slag	Mean	66.7	Collé et al., 1981
Slag from copper-slate	Mean (range)	1500 (860 – 2100)	BFS, 2024
Soil	Mean	10.0	Collé et al., 1981
Gravel, sand, gravel sand	Mean (range)	15 (1 – 39)	BFS, 2024
Concrete	Mean (range)	30 (7 – 92)	BFS, 2024